Tomas Bata University in Zlín
Faculty of Technology

Doctoral Thesis Summary

Curing of Visible Light Curing Resin Based Dental Composites

Vytvrzování dentálních materiálů

Author:	Thomas Haenel MSc
Degree programme:	P2808 Chemistry and Materials Technology
Degree course:	2808V006 Technology of Macromolecular Substances
Supervisor:	Prof. Ing. Berenika Hausnerová, Ph.D.
External examiners:	Prof. Ing. Ivan Hudec, PhD.
	doc. Ing. Petr Humpolíček, Ph.D.
	Ing. Vladimír Pelíšek, Ph.D.

Zlin, September, 2016

Published by **Tomas Bata University in Zlín** in the Edition **Doctoral Thesis Summary.**
The publication was issued in the year 2016

Key words in Czech: *Klíčová slova: fotokompozit, vytvrzování světlem, dielektrická analýza, kinetika vytvrzování, distribuce záření, tvrdost, viskoelastické vlastnosti.*

Key words in English: *visible light curing resin based composites, photo-polymerization, dielectric analysis, reaction kinetics, light distribution, hardness testing, viscoelastic properties.*

Full text of the Doctoral thesis is available in the Library of TBU in Zlín. (14 pt)

ISBN 978-80-……

ABSTRACT

During the last 50 years, a broad range of visible light curing resin based composites (VLC RBC) was developed for restorative applications in dentistry. Correspondingly, the technologies of light curing units (LCU) have changed from UV to visible blue light, and there from quartz tungsten halogen over plasma arc to LED LCUs increasing their light intensity significantly.

In this thesis, the influence of the curing conditions in terms of irradiance, exposure time and irradiance distribution of LCU on reaction kinetics as well as corresponding mechanical and viscoelastic properties were investigated.

Different experimental methods were used to determine time dependent degree of conversion (*DC*), depth of cure (*DoC*), hardness distribution and post-curing kinetics. Dynamic mechanical indentation technique was implemented on a dynamic mechanical analyzer to determine local viscoelastic properties on a scale of 100 to 300 µm.

To evaluate the data several quantitative approaches were applied. A novel *DC*-function based on a time dependent reaction constant is presented to produce intrinsically final *DC*-values less than 100 % and better representation *DC*-data. The novel *DC*-function shows that the kinetics of the curing reaction is mainly determined by the reaction time constant which depends on the irradiance of the LCU. The *DC* reached 45 % after time corresponding to the reaction time constant. It was shown that the reaction rate depends on the square root of irradiance for the investigated composites.

A new method to determine *DoC* in a user-independent and automatized manner was presented which can be applied to any depth dependent property of light curing composites. Due to the mathematical description, the properties at *DoC* have decreased to 88 % of their plateau values, and are thus not arbitrary.

Furthermore, the irradiance distribution of the LCU is reflected in the distribution of mechanical properties. Longer exposure times increase the hardness level, but do not level out the imprinted patterns. This is in accordance with long term hardness measurements revealing that the kinetics of the post-curing has a logarithmic time dependency, and is also determined by the locally introduced irradiance. Samples irradiated with different exposure times produced hardness curves which could be shifted to a master curve on the logarithmic time axis allowing for long term predictions of the hardness, and indirectly the *DC*.

RESUME

Reaction kinetics and resulting mechanical and viscoelastic properties of visible light curing resin based composites (VLC RBC) at various curing conditions are investigated. A novel degree of conversion (*DC*) function was determined, providing improved representation of *DC*-data. Further, this *DC*-function shows that the kinetics of the curing reaction is mainly determined by the reaction time constant which depends on the irradiance of the light curing units (LCU) under examination. The irradiance distribution of the LCU is reflected in the distribution of mechanical properties. Longer exposure times increase the hardness level, but do not level out the imprinted patterns. Samples irradiated with different exposure times produced hardness curves which could be shifted to a master curve allowing for long term predictions of the hardness, and indirectly the *DC*. A new method to determine depth of cure in a user-independent and automatized manner was presented which can be applied to any depth dependent property of light curing composites.

FAZIT

Diese Studie befasst sich mit der Reaktionskinetik und den resultierenden mechanischen und viskoelastischen Eigenschaften von lichthärtenden Dentalkompositen (VLC RBC) in Abhängigkeit der Belichtungsbedingungen. Während dieser Studie wurde eine neue Umsatzfunktion entwickelt, die zu einer Verbesserung der Darstellung der Umsatzdaten führt. Anhand dieser Funktion kann gezeigt werden, dass die Reaktionskinetik hauptsächlich durch die Reaktionszeitkonstante bestimmt wird, die vor allem von der Intensität der verwendeten Belichtungslampen abhängt. Die Intensitätsverteilung der Belichtungslampen spiegelt sich in der Verteilung der mechanischen Eigenschaften der Dentalkomposite wieder. Eine Verlängerung der Belichtungszeit führt dabei zu einer Steigerung der Härte, allerdings nicht zu einem Ausgleich der ungleichmäßigen Verteilung der mechanischen Eigenschaften. Die Belichtung von Proben mit unterschiedlichen langen Zeiten liefert Härteverläufe, die über die Verschiebung zu einer Masterkurve, die Vorhersage von Härteverläufen über einen längeren Zeitraum ermöglichen. Eine neue Methode wurde zur automatischen und benutzerunabhängigen Bestimmung der Aushärtetiefe entwickelt. Dies neue Methode kann auf verschiedene tiefenabhängige Eigenschaften von Dentalkompositen angewendet werden.

CONTENTS

1 STATE OF THE ART

1.1 Dental composites

The visible light curing resin based dental composites (VLC RBC) are the mostly used material in the dentistry practice today. They are used e.g. as restoration, crown material, inlays or root canal posts [1]. The development of the dental material was started in the 1950s with self-curing materials [2]. From the middle of the 1960s to the middle 1970s the light curing composite initiation changed from UV-light curing to visible light curing, which is safer in the application due to ozone generation and radiation damages caused by UV-light [3,4]. The LED curing technology is state of the art of the light curing units today. Energy efficiency, easy handling and long lifetime are the main advantages of this technique.

1.1.1 Composition of VLC RBCs

The VLC RBCs consist of three main components, the monomer system, the initiator system and the fillers. The first part, the monomer system, is an organic system building the polymer matrix during the photo-polymerization process. The most common monomers are bisphenol A glycidyl methacrylate (Bis-GMA), ethoxylated bisphenol-A dimethacrylate (Bis-EMA), urethane dimethacrylate (UDMA) and triethylene glycol dimethacrylate (TEGDMA) [5–7]. The monomer matrix defines the different properties of the VLC RBCs in uncured and cured state by adjusting the viscosity, light transmission by refraction index or the volume contraction during polymerization.

The second part is the initiator system. The function of the VLC RBC initiator system is the conversion of light energy from the LCU into a radical state of the initiator molecules to start the photo-polymerization. The commonly used initiator systems are composed of camphorquinone (CQ) and ethyl 4-(dimethylamino) benzoate (DABE) [3]. For bleaching products, that need to be colorless, monoacylphosphine oxid (TPO) or 1-phenyl-1,2-propandedione (PPD) are used, [1,4,8].

The third part of the VLC RBCs is the filler system. The filler consists of an inorganic material - typically grinded glass or minerals [1,9–11]. The main function of fillers is the improvement of physical and mechanical properties of VLC RBCs, e.g. increasing stiffness, reducing shrinkage during polymerization or improving handling properties [12]. The properties are adjusted by variation the size from the micro- to the nanoscale (50 µm to 0.005 µm) and/or the amount of fillers (50 wt% up to 85 wt%) [1,9,10,13]. New developments such as pre-polymerized fillers (PPF) improve final properties such as the shrinkage bounding or the polishability [12].

1.2 Photo-polymerization process

The photo-polymerization process is a radical, chain-growth polymerization, which is divided in three processes: initiation, propagation and termination [11,14]. The initiation process is started by irradiation of light that transfers CQ to an exited energy state. In this excited state it can react with a DABE molecule to active amino alkyl radicals [3,15–17]. After the light activation, the initiator molecules form radicals ($R^{\bullet}$) and start the polymerization process with monomers.

Start reaction: $$A\bullet + DMA \xrightarrow{k_{start}} A-(DMA)\bullet \quad \text{(I)}$$

Growth reaction: $$A-(DMA)_n-(DMA\bullet) + DMA \xrightarrow{k_{ucg}} A-(DMA)_{n+1}-(DMA\bullet)$$

1.2.1 Reaction kinetics of the overall polymerization process

The main topic of this work is the investigation how the viscoelastic properties are affected by the curing conditions. Also a more detailed view on the reaction kinetics, the degree of conversion (*DC*) and depth of cure (*DoC*) is presented. In the "steady state" initiation and termination are in equilibrium, the overall rate of reaction R_{pol} is Eq. (1) [18]:

$$R_{pol}(t) = \frac{d[M]}{dt} = -\frac{k_p}{k_t^{0.5}}[M](\phi I_0 e^{-\varepsilon c x})^{0.5} \quad (1)$$

The time and depth depending $DC(t,x)$ is determined by integration of Eq. (2):

$$DC(t,x) = 1 - \frac{[M](t,x)}{M_0} = 1 - e^{-\frac{k_p}{k_t^{0.5}}(\phi I_0 e^{-ax})^{0.5} t} \quad (2)$$

The *DC* is an important measure to characterize the curing behavior of VLC RBCs and can be determined by spectroscopic methods, such as FTIR and Raman spectroscopy, thermal analysis e.g. differential scanning calorimetry (DSC) or dielectric analysis (DEA) [14,19–22]. The *DoC* can be determined using mechanical methods (hardness tests, ISO 4049 scratch test or nanoindentation [23–26].

1.3 Methods to determine curing state and degree of conversion

1.3.1 Infrared spectroscopy

The attenuated total reflection Fourier transform infrared spectroscopy (ATR-FTIR) is used to trace the polymerization process of VLC RBCs [22,27,28]. Samples with defined thickness are placed above a crystal and the IR beam penetrates few microns as an evanescent wave [29], Fig. 1.

During the polymerization, the molecular structure, and therefore the absorbance (*Abs*) of the specimen, change as the number of aliphatic C=C bounds decreases. The time dependent $DC_{IR}(t)$, can be calculated by the following equation:

$$DC_{IR}(t) = \frac{\left\{\frac{\left[[Abs_{aliphatic}](t)\right]}{[Abs_{aromatic}]}\right\}_{polymer}}{\left\{\frac{[Abs_{aliphatic}]}{[Abs_{aromatic}]}\right\}_{monomer}} \quad (3)$$

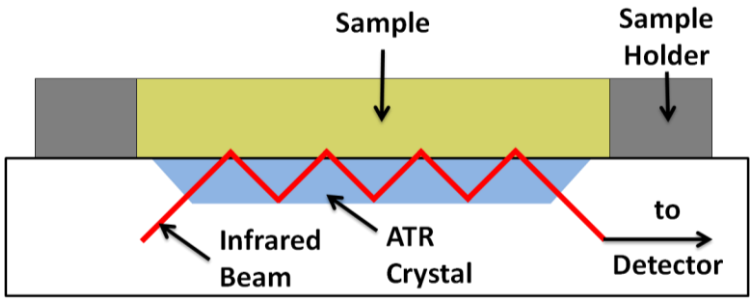

Fig. 1 Principle of ATR-spectroscopy [30]

1.3.2 Raman Spectroscopy

Raman spectroscopy is a complementary technique to IR-spectroscopy to determine the *DC* of VLC RBCs [26,31–35]. This method is based on the inelastic light scattering on molecules and the resulting shift in energy by delivered or absorbed energy of the photons (Stokes- and anti-Stokes scattering) [31,32].

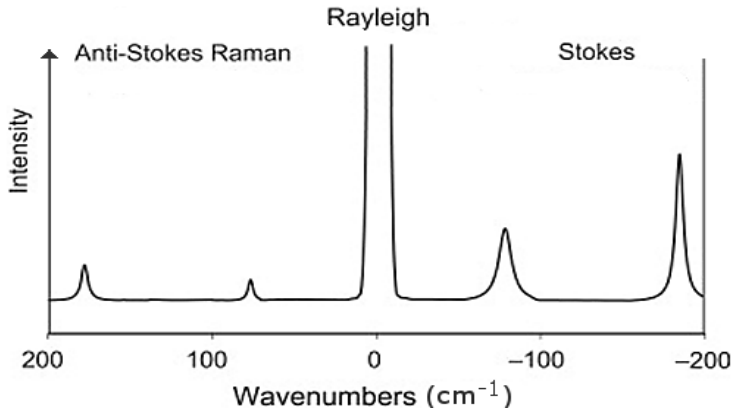

Fig. 2 Comparison of anti-Stokes and Stokes peak intensities with respect to the Rayleigh peak intensity [31]

Fluorescence caused by ingredients of the VLC RBCs can overlap with the Raman scattered light [20,35]. Furthermore, laser light absorption increases the sample temperature and may cause thermal degradation [36].

1.3.3 Differential scanning calorimetry

The differential scanning calorimetry (DSC) allows for determining the heat flow $\dot{Q}$ between sample and environment being proportional to the reaction rate [37–39]. The time dependent $DC_{DSC}(t)$ can be defined by evaluating the peak of curing enthalpy in the following way, Eq. (4):

$$DC_{DSC}(t) = \frac{\int_{t_{start}^{peak}}^{t} \dot{Q}(t')dt'}{\int_{t_{start}^{peak}}^{t_{end}^{peak}} \dot{Q}(t')dt'} = \frac{\int_{t_{start}^{peak}}^{t} \dot{Q}(t')dt'}{\Delta Q_{curing}} \quad (4)$$

with the heat flow $\dot{Q(t)}$ and curing heat ΔQ_{curing} [40] given by the nominator integral. Additionally, post-curing processes caused by trapped radicals in the cured resin can be characterized by the post-reaction enthalpy [41,42].

1.3.4 Dielectric analysis

The dielectric analysis (DEA) [43] allows for the monitoring the change of dielectric properties of VLC RBCs during the curing process [44,45]. The high data acquisition rate at high frequencies allows real-time monitoring of fast curing processes of VLC RBCs as well as a long-time observation [45,46]. With ongoing curing of a VLC RBC the network density increases, and as a result, the ion viscosity $\eta^{ion}(t)$ increases too, because of the restricted ion mobility. The assumption $\eta^{ion}(t) \sim DC(t)$ allows for the calculation of $DC_{DEA}(t)$, Eq. (5):

$$DC_{DEA}(t) = \frac{\eta^{ion}(t) - \eta_0^{ion}}{\eta_\infty^{ion} - \eta_0^{ion}} \quad (5)$$

with the initial ion viscosity η_0^{ion} and the final ion viscosity η_∞^{ion}.

1.4 Determination of viscoelastic properties of VLC RBCs using indentation methods

Indentation methods such as hardness testing or nanoindentation allow for the determination of local mechanical properties, Table 1, and as a consequence the influences of curing conditions e.g. irradiance or exposure time on the properties of the VLC RBCs. In dental material science, indentation methods are used to compare hardness with other properties such as *DC*, *DoC* or to map the surface hardness distribution for mechanical imaging [23,47–49].

Table 1 Indentation methods and measured variables of mechanical methods to determine the mechanical and viscoelastic properties of VLC RBCs

Method	**measurable quantities**	**spatial resolution**
Hardness tester	Hardness, depth of cure	local
Atomic force microscopy	Stiffness, surface roughness	local
Nanoindenter	Stiffness, hardness, depth of cure	local

1.4.1 Instrumented indentation techniques

Instrumented hardness tester, nanoindenter and atomic force microscopy (AFM) determine force-indentation vs. depths curves providing significantly more material information such as hardness, plastic deformation energy, creep and relaxation properties and Young's modulus. The determination of the elastic modulus is based on the work of Oliver and Pharr [50]. The loading curve is followed by an unloading curve, whereas the linear section of the unloading curve is used to determine Young's modulus. The slope of the linear section is called "stiffness" and is a measure for the elasticity of a material with the contact area of the indenter *A*.

$$S = \frac{dP}{dh} = \frac{2}{\sqrt{\pi}} E \cdot \sqrt{A} \tag{6}$$

The determined elastic modulus depends on moduli and Poisson's ratios of both tip (E_t, ν_t) and sample (E_s, ν_s).

$$\frac{1}{E} = \frac{1-{\nu_s}^2}{E_s} + \frac{1-\nu_t^2}{E_t} \tag{7}$$

1.4.1.1 Atomic Force Microscopy (AFM)

The AFM allows for the determination of surface properties on a nanoscale (0.1 to 10 nm), using repulsive and attractive atomic forces of surface atoms and atoms of a fine tip [51–55]. AFM indentation can be used to map local mechanical properties of a surface. AFM consists of a cantilever spring with defined stiffness and a fine tip at the end, a laser diode, a position sensitive photo-detector, a xyz-stage for 3D positioning and a processing unit. The position of the cantilever spring tip is determined by the position of the reflected laser beam on the photo-detector [53]. The cantilever spring bends during the indentation and its deflection is detected by the laser beam. As the cantilever stiffness is known the applied load *P* can be calculated by the displacement of the cantilever spring.

1.4.1.2 Nanoindenter

The nanoindenter is an instrumented indentation technique to measure mechanical properties in the force range of 40 and 1800 mN with lateral resolution of >10 nm [56–58]. Nanoindenters are equipped with motorized xy-stage for mechanical images and use the typical hardness indenter geometries e.g. Vickers, or Berkovich [56]. Furthermore, the nanoindenter can measure in dynamic mechanical modes, which allow to measure viscoelastic properties [56].

Most applications for nanoindenters in dental material science are the determination of hardness and elastic modulus depending on curing conditions. They are compared with other material properties, such as *DC* or the influence of morphology or composition of VLC RBCs [59–63]. Due to the high resolution the determination of small spatial characteristics such as the influence of coupling agents on the mechanical properties is possible [64].

1.4.2 Mechanical imaging and mapping

The great advantage of instrumented indentation techniques is the automation of measurement and data acquisition as well as data evaluation for mechanical mapping, Fig. 3. Mechanical mapping visualizes differences in local mechanical properties of a surface, e.g. caused by filler particles or inhomogeneous curing [47,49,65]. This is especially used in dental material science to determine the effects of light intensity distribution of the LCU on the mechanical properties of cured VLC RBCs [47,49].

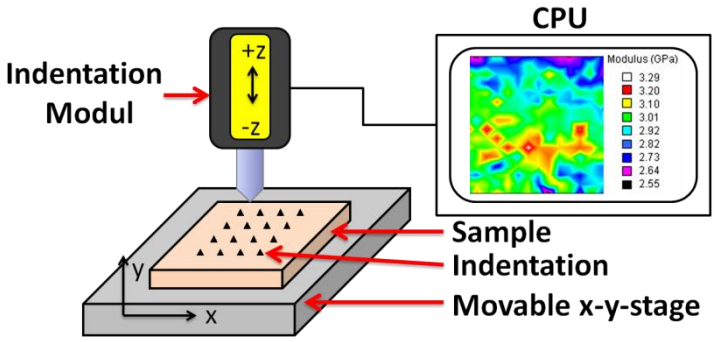

Fig. 3 Scheme of a mapping system to determine the mechanical property distribution of a sample surface.

1.5 Dynamic mechanical Analysis (DMA)

The dynamic mechanical analysis (DMA) is a method to characterize the viscoelastic behavior of materials in terms of the temperature and frequency dependent complex modulus $E^*(\omega,T)$ [39,66,67]. Besides, the determination of $E^*(\omega,T)$ further mechanical properties are provided such as storage E', loss modulus E'', loss factor tan $\delta(\omega)$ and glass temperature T_g. As mechanical properties change drastically during a phase transition, transition temperatures can be determined very sensitively. Additionally, DMA measurements are used to determine the frequency and temperature depended behavior to construct master curves, Fig. 4 [66,67]. They allow for predicting material behavior beyond the experimentally accessible measuring range, e.g. high frequency performance of tire rubbers [68] or long time behavior of plastic pipes [69].

In the field of dental composites, the DMA is used to determine the stiffness of VLC RBCs after curing to evaluate the influence of the curing conditions [70–73]. Another application is the investigation of the kinetics of post-curing processes. As post-curing happens slowly, DMA with low frequencies (< 1 Hz) reveals a logarithmic time dependency of the post-curing process.

Besides the characterization of the bulk viscoelastic behavior, DMA allows for the determination of local viscoelastic properties in the compression mode with small size indenters [74]. Therefore, it is principally possible to determine local mechanical properties for the VLC RBCs comparable with nanoindentation.

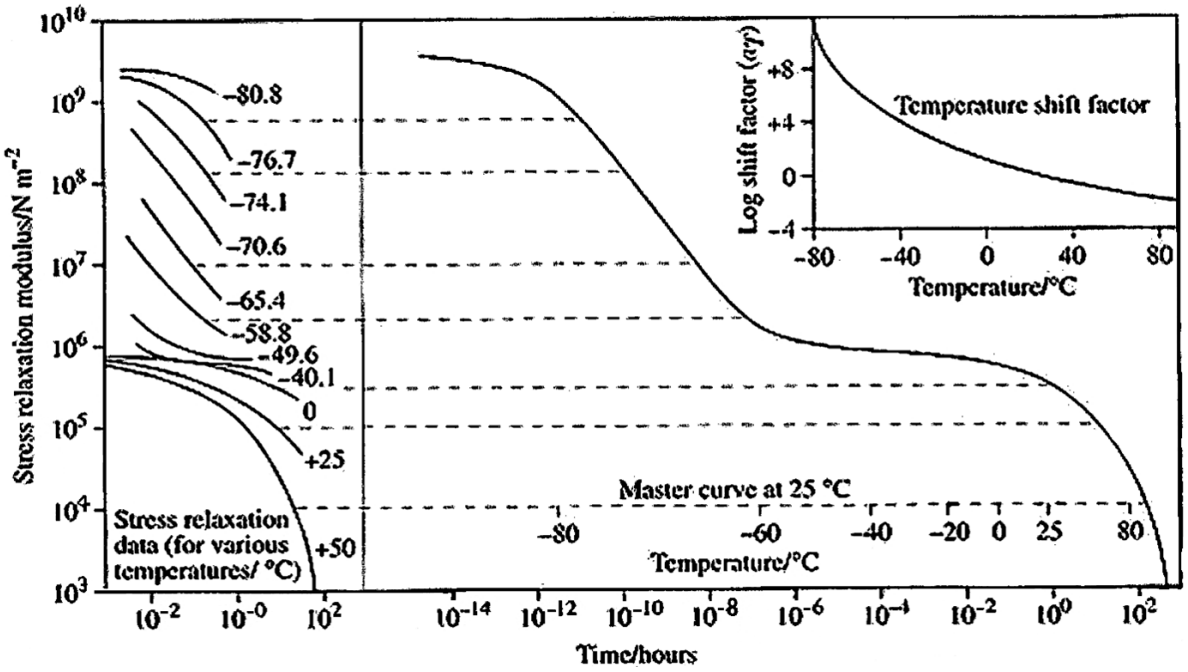

Fig. 4 Construction of the master curve for PIB at 25 °C reference temperature by shifting stress relaxation curves obtained at different temperatures horizontally along the time axis. The shift factor a_T varies with temperature as shown [75].

2 METHODOLOGY AND PURPOSE OF THE WORK

Visible light curing resin based dental composites (VLC RBCs) are the most common used dental restorative materials. These materials were developed to replace amalgam based restoratives first because of elution of mercury, which may cause health problems, and second, in order to improve esthetic aspects/requirements of patients. The resulting material properties and the life time of VLC RBCs depend on the curing conditions. The main influence factors on the resulting material properties are irradiance, light distribution and spectrum of the light curing unit (LCU). The methods employed in this work shall provide information about LCU characteristics, mechanical as well as curing parameters, e.g. degree of conversion (*DC*), time dependent *DC* (*DC*(*t*)), depths of cure (*DoC*) and hardness of the VLC RBC, Fig. 5.

Until now there is no model established which can predict sufficient *DC* and *DoC* dependences on curing conditions such as irradiance or exposure time. Furthermore, there is hardly any knowledge about the influence of curing conditions on post curing, thus predictions of the surface hardness cannot be made. Generally, it is known that the LCUs emit inhomogeneous light, and therefore the curing will be inhomogeneous, e.g. surface hardness distribution. No one knows how curing conditions, such as irradiance and exposure time, influence the resulting distribution of the mechanical properties. Often, materials show inhomogeneous mechanical properties, e.g. hardness inhomogenities induced by light distribution. A dynamical mechanical analysis (DMA) has an ability to determine viscoelastic properties of materials. Unfortunately, a micro-indentation system for a commercial DMA is not available yet.

Kinetic models are necessary to predict the *DC*(*t*) and *DoC*. The kinetic models will have to be adjusted with measured *DC*(*t*) and *DoC* results for different curing conditions. To determine *DC*(*t*) for different curing conditions a Fourier transform infrared spectroscopy (FTIR) is used in this work. *DoC* will be measured by using differential scanning calorimetry (DSC), hardness and mass loss in strong solvent. To gain more information about the influences of the curing conditions on post curing, a master curve based superposition will be proposed. The surface hardness for VLC RBCs under different curing conditions will be measured at different times with hardness testing. Different LCUs will be characterized by ultra violet visible spectrometer (UV-Vis) for irradiance and spectra, and a laser beam profiler will be utilized for light distribution. These data will be used to compare the LCU characteristics to the distribution of the local mechanical properties of VLC RBCs measured by mechanical imaging with hardness testing.

For the development of a micro-indentation DMA an indenter system with sample holder and movable x-y stage will be adapted to the DMA to allow the determination of viscoelastic properties. A validation of this indentation method will be done by comparing the moduli measured in DMA three point bending mode with those measured in an indentation mode. The results of the mechanical imaging using DMA microindentation will be compared with the results from Knoop hardness mapping.

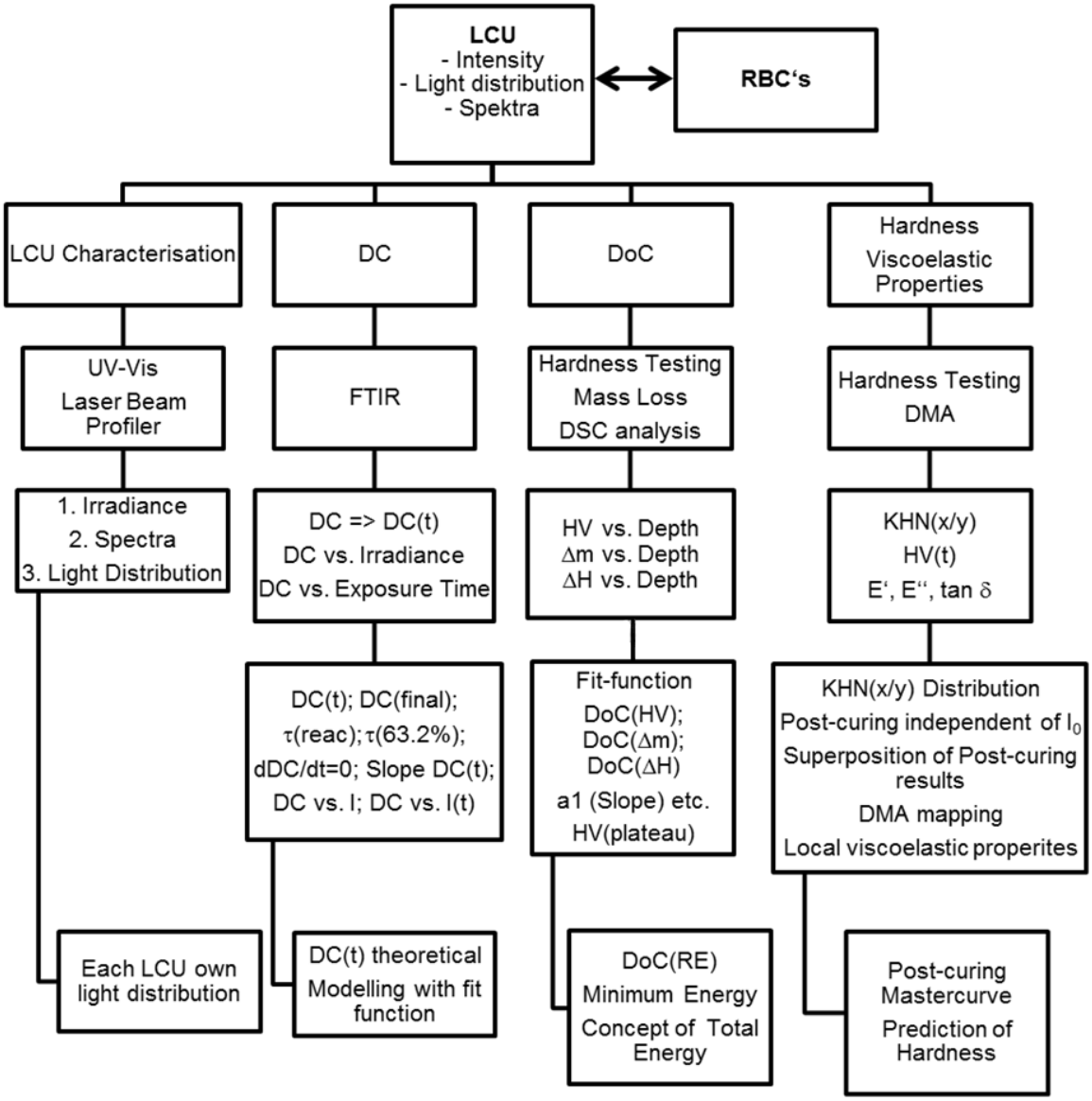

Fig. 5 Flow chart of the plant methodology and methods of the PhD thesis

3 DISCUSSION OF THE RESULTS

3.1 Characterization of dental light curing units

The mechanical and chemical properties depend on the *DC* of the VLC RBC [76–79]. Therefore, the emission spectra, irradiance and irradiance distribution were measured with an integrated sphere, laser power meter and laser-beam profiler to compare them with the properties of the VLC RBCs.

3.1.1 Light energy and spectral measurements [P-I and P-VI]

Each LCU shows an individual spectrum and irradiance level and in respect to the effective absorbance wavelength of CQ (~ 460 nm), the differences may lead to differences in the curing performance [80,81], [P-I Table 1].

The measurement of the absorbance energy through an increasing thickness of a VLC RBC sample shows an exponential decrease, [P-VI Fig. 3]. It was shown that the reflection of light energy on the sample surface is approximately 30 %.

3.1.2 Light distribution measurements [P-I]

Measurements of irradiance distributions by a laser-beam profiler show that each LCU has an individual irradiance distribution pattern, Fig. 6, due to the internal setup [82]. The inhomogeneous irradiance distribution with high and low intensity areas may lead to insufficient curing of restorations.

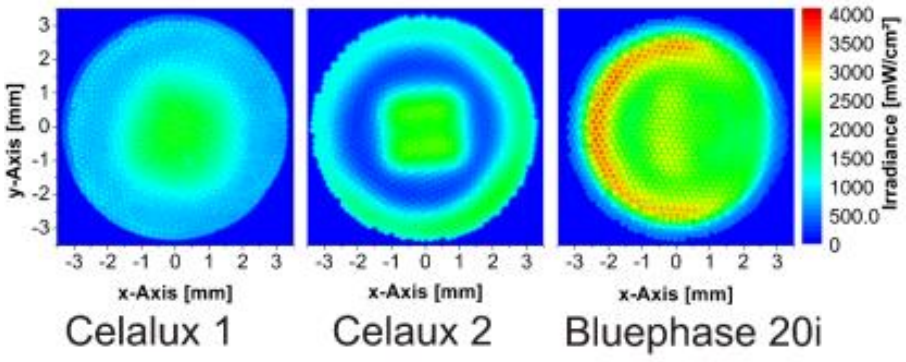

Fig. 6 Laser-beam profiler images of Celalux 1, Celalux 2 and Bluephase 20i in Turbo Mode

The comparison of the laser-beam profiler, the single lens reflex (SLR) and the iPad measurements show similar intensity distribution results thus helping dentists to gain quick information on the intensity distribution of LCUs.

3.2 Kinetics of VLC RBCs

3.2.1 Modelling reaction kinetics of VLC RBCs [P-II]

For the first seconds of the curing the time dependent *DC* can be described with Eq. (12) which is the primary curing in the liquid state [46,83]:

$$DC(t) = 1 - \frac{c^{DMA}(t)}{c_0^{DMA}} = 1 - e^{-\frac{t}{\tau_{reac}^0}} \tag{12}$$

c_0^{DMA} = concentration of DMA molecules at the beginning

t = curing time

$c_0^{DMA}(t)$ = concentration of DMA molecules at a certain time

τ_{reac}^0 = reaction time constant

Eq. (12) produces a final *DC* of 1 whereas *DC*-values between 0.5 and 0.7 are experimentally found [19,22,84,85]. Therefore, a novel *DC*-function based on a time dependent reaction constant was derived providing a correction term $K(t)$ limiting the *DC*-values to less than 1 (or 100 %), Fig. 7.

$$DC(t) = 1 - \frac{c^{DMA}(t)}{c_0^{DMA}} = 1 - e^{-\frac{t}{\tau_{reac}^0{}'}} * \underbrace{\left(\frac{\tau_{reac}^0 + \Theta * e^{\frac{t}{\tau_{grow}}}}{\left(\tau_{reac}^0{}' + \Theta\right)} \right)^{\frac{\tau_{grow}}{\tau_{reac}^0{}'}}}_{\text{correction term } K(t)} \tag{13}$$

with $\tau_{reac}^0{}'$ constant part of reaction time constant in the liquid phase

τ_{grow} growing time constant

Θ strength of the time dependent part

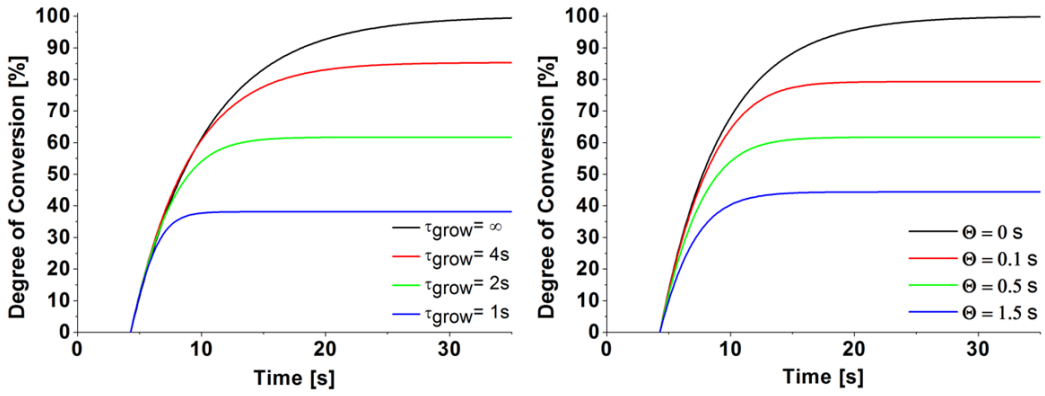

Fig. 7 Effect of growing time constant τ_{grow} and strength Θ on DC-curves [P-II].

The novel *DC*-function produces a good correlation with the measured data in the initial phase of the reaction (15 s fit interval), [P-II Fig. 5]. The reaction time constants τ_{reac}^0 decreased by a factor of 1.9 (Arabesk) and by a factor of 1.8 (Grandio), if the irradiance is increased by a factor of 3.3. This factor is comparable

with the results of the direct method. Fig. 8 shows that the reaction rate constants τ^0_{reac} depends reciprocally on the square root of the irradiance and are fitted well with

$$\tau^0_{reac}(I_{LCU}) = \frac{a}{I^b_{LCU}} \tag{14}$$

The parameter "*b*" of the potential fit function is close to -0.5 for both Arabesk and Grandio. This confirms the predicted irradiance dependency of reaction rates for the photo-polymerization of VLC RBCs [18].

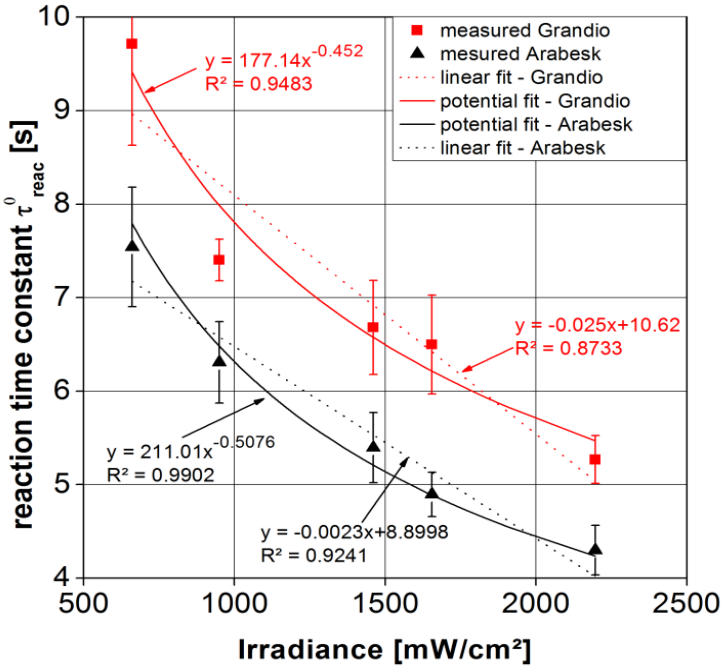

Fig. 8 Dependency of reaction time constant on the irradiances of LCU

3.2.2 Evaluation of the DC and total energy concept [P-III]

The basic idea of "total energy concept" or "exposure reciprocity" is that achieved *DC* of VLC RBCs depends only on equivalent amounts of energy irrespective of LCU irradiance or exposure time [86,87]. It is often used to choose the best exposure strategy for curing.

Real time measurements of *DC* were performed by FTIR-ATR, [P-III Fig. 2]. The samples were irradiated with a radiant exposure of approximately 18 J/cm² with different irradiance levels and corresponding exposure times. The results were fitted by a function considering the primary curing (exponential term) in the liquid state at the beginning, and the post-curing (logarithmic term) considering the curing in the glassy state of the VLC RBC, Eq. (15):

$$DC(t) = \underbrace{A \cdot \left(1 - e^{\left(-\frac{t - t_{LCU}}{\tau^0_{reac}}\right)}\right)}_{primary\,curing} \cdot \underbrace{\left(1 + B \cdot \ln\frac{t}{t_{LCU}}\right)}_{post-curing} \qquad (15)$$

with t_{LCU} time at which the LCU was switched on
A fit parameter, achievable *DC* of primary curing
B fit parameter, increase of *DC* due to post-curing

DC-curves, Fig. 9 (left), show an increase of the initial slope corresponding to a decrease of τ^0_{reac} for higher. If *DC* is plotted versus total energy, the *DC*-curves do not coincide, Fig. 9 (right). Consequently the total energy concept fails at least for high irradiances although the *DC* after 170 s was equal for all *DC*-curves.

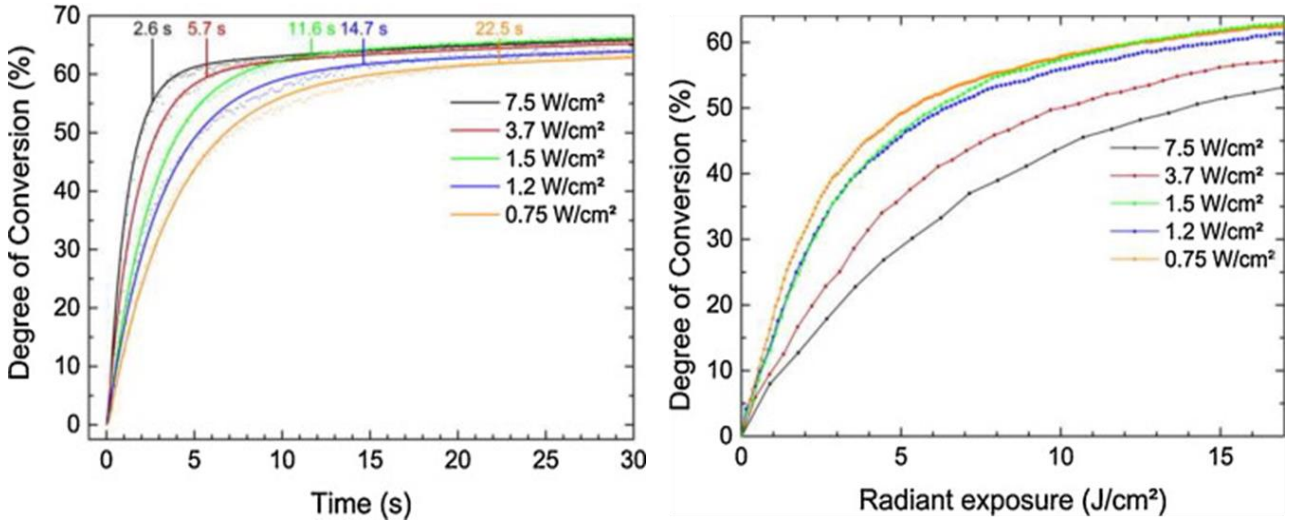

Fig. 9 left: Comparison of DC_{exp} and DC_{fit} curves of Tetric EvoFlow irradiated with 19 J/cm²; right: DC_{exp} as a function of radiant exposure (J/cm2) [P-III].

3.3 Effects of curing condition on the properties of VLC RBCs

3.3.1 Effects of the curing time and irradiance on the depth depending properties [P-IV]

The effects of irradiance and exposure time on hardness, mass loss in THF and post reaction enthalpy were investigated depth for two VLC RBCs. The depth dependent properties were evaluated using a fitting procedure. For details of the measuring as well as evaluation procedures, see Fig. 10 and [P-IV].

Due to the sigmoidal shape of the curves a hyperbola tangent is used to fit the depth dependent data (lines in Fig. 10). For the hardness data it is given by Eq. (16):

$$HV(x) = \frac{HV^{Plateau}}{2} \cdot \left\{1 + tanh\left[-a_1\left(x - x_{0,1}\right)\right]\right\} \qquad (16)$$

with HV hardness
x depth
a_1 slope at inflection point
$x_{0,1}$ depth of inflection point

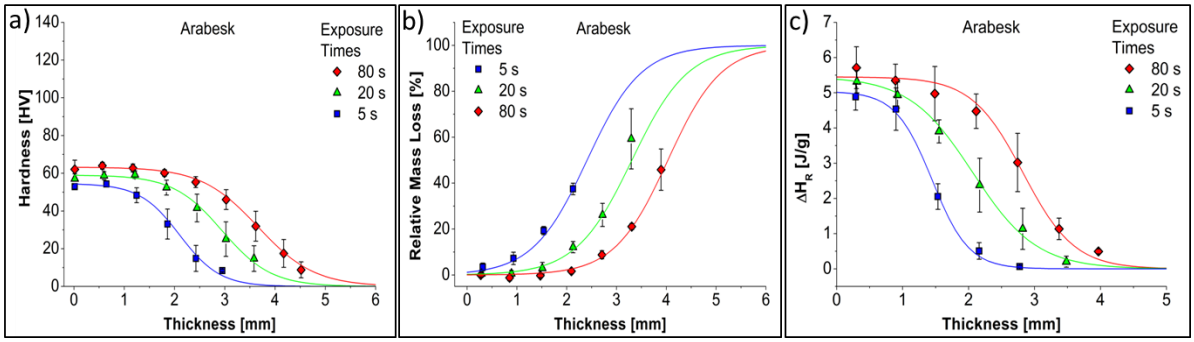

Fig. 10 Depth depending hardness a), mass loss b) and post-reaction enthalpie ΔH_R c) vs. sample thickness of Arabesk Bluphase 20i Turbo mode.

The advantage of this fit function is that it takes into account all measured data, thus being user-independent. Furthermore, it leads to a new definition of the depth of cure (DoC_{HV}) given by the relationship, Eq. (17):

$$DoC_{HV} = x_{0,1} - \frac{1}{a_1} \qquad (17)$$

Graphically it is the depth at which the plateau value intercepts the slope at the inflection point, Fig. 11.

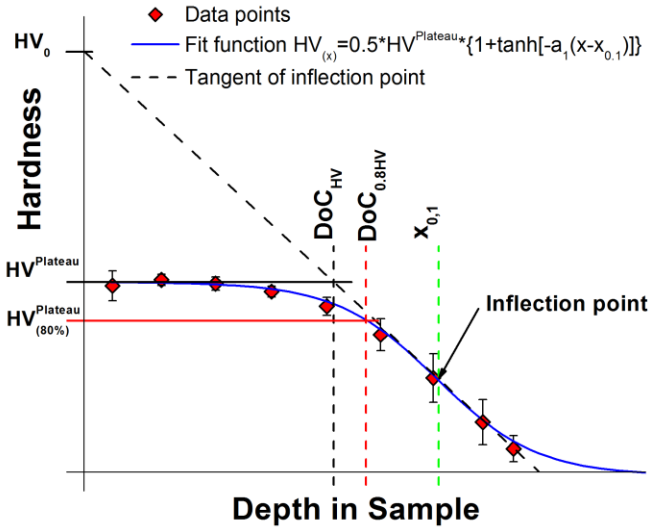

Fig. 11 Scheme of the evaluation of depth dependent hardness data using Eq. (16)

Established methods e.g. ISO 4049 scratch test or 80 % of plateau hardness are single point methods and overestimate *DoC* compared to Eq. (16). The introduction of DoC_{HV} to Eq. (16) shows that the hardness dropped to 88 % compared to the plateau value. The correlation of DoC_{HV} and radiant exposure (*RE*) reveals a logarithmic dependency, Fig. 12.

$$DoC_{HV}(RE) = A * \ln RE + B \quad (18)$$

with the parameters A and B describing materials properties of VLC RBC. The reduction of light intensity with depth due to Beer-Lambert-absorption law leads to the consequence that *DoC* is limited because no light will come to depth exceeding 5 times the penetration depth, and the energy introduction cannot be increased at will because of the risk of tissue damage by irradiation. The evaluation also shows that a minimum radiant exposure of around 0.5 J is needed to overcome effects caused by inhibition.

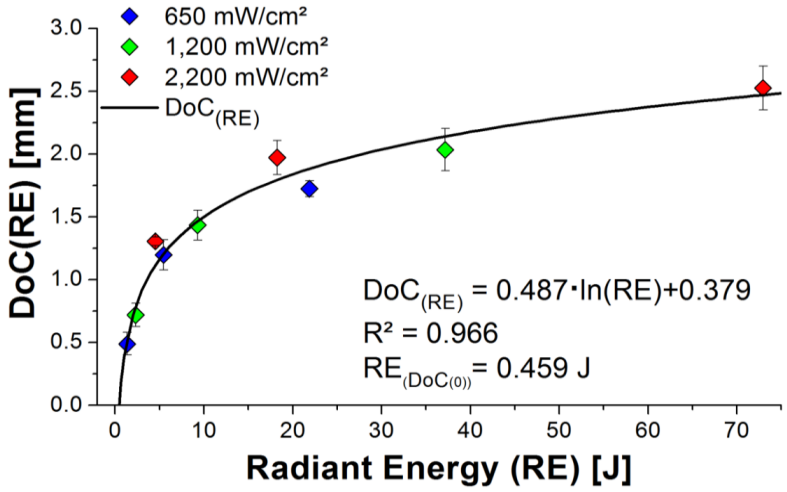

Fig. 12 DoC vs. radiant energy (RE) (Arabesk)

3.3.2 Effects of irradiance distribution on the mechanical surface properties [P-V]

Due to their design, LCUs produce different patterns of irradiance distribution, [P-V Fig. 4]. This leads to locally different *DCs* and thus different mechanical properties reflected in the hardness distributions of the samples, Fig. 6.

The increase of the exposure time leads to an increase of the hardness values. Therefore, one may expect that an increase of exposure time should also increase the hardness and compensate for irradiance distributions of LCU in the long term. However, areas exposed with low irradiances are always found to have lower hardness values compared to areas exposed with high irradiances, irrespective of exposure time. A homogenization with increasing exposure time does not take place. An imprinted irradiation pattern is conserved it the T_g exceeds ambient temperature.

The formation of a crosslinked polymer network during photo-polymerization is a fast process. The reaction rate reaches the maximum after a few seconds, [P-V Fig. 6], and the structure of the crosslinked polymer network is frozen, inhibiting compensation processes because of the inhibited mobility in the glassy state. Therefore, it can be concluded that the “total energy concept” is only applicable for bulk and not for local properties.

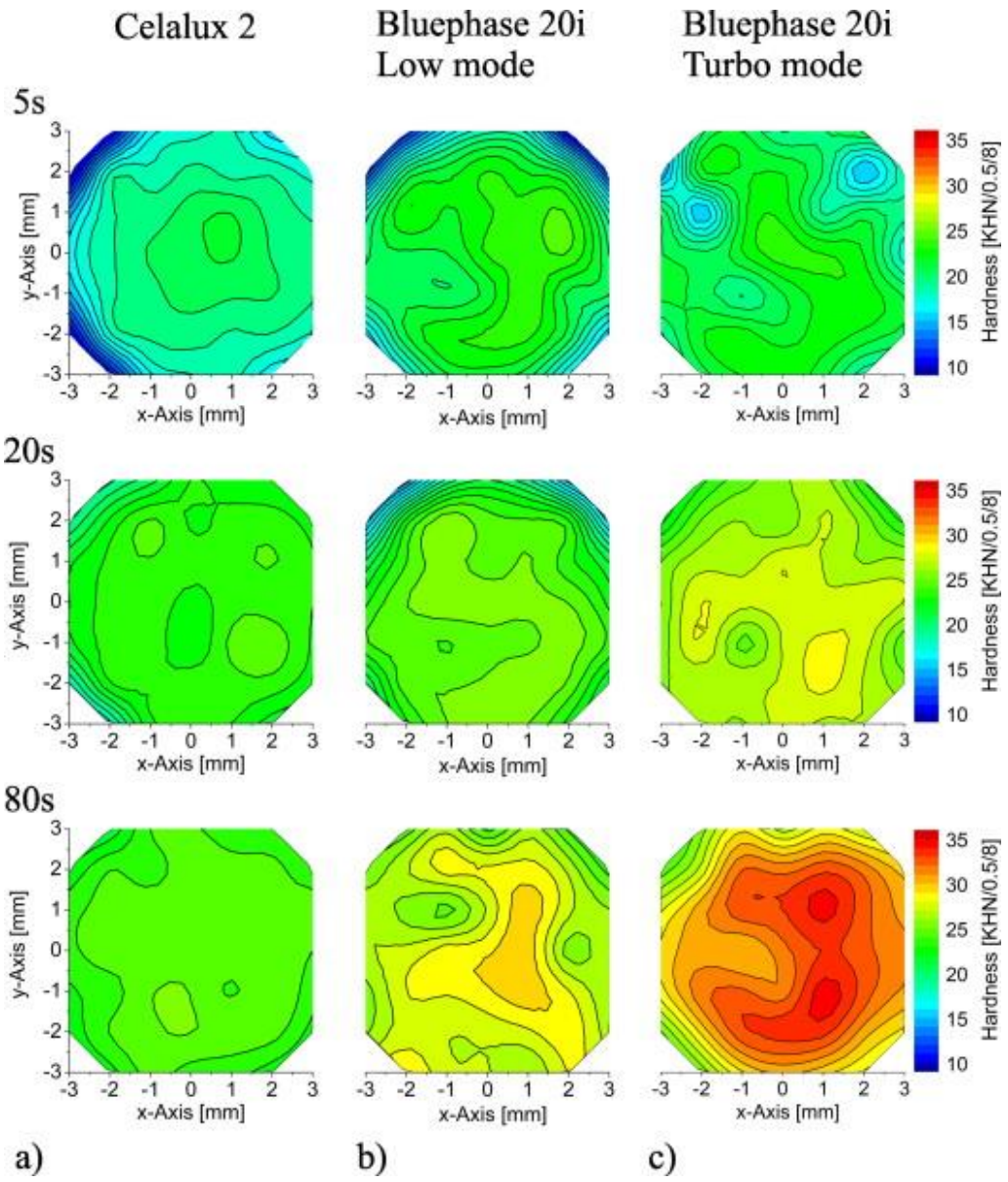

Fig. 13 Surface hardness distributions of Arabesk specimens after 5, 20 and 80 s exposure time using the Celalux® 2 (a), Low mode (b) and Turbo mode (c).

3.3.3 Development of a dynamic mechanical indentation method to determine local viscoelastic depth and surface properties of VLC RBCs [not published yet]

Dynamic mechanical analysis (DMA) provides information about the viscoelastic properties with respect to time, temperature and frequency. A commercial DMA requires relatively large samples, and therefore determines bulk properties. This can be overcome if DMA is modified to a dynamic mechanical micro-indenter allowing for determining viscoelastic properties locally. To modify DMA two approaches were necessary:

1. Indenter holders for a high lateral resolution (a tungsten needle) and for lower lateral resolutions (Vickers, Berkovich and Rockwell indenters) were adapted to the DMA, Fig. 22.

2. A XY-movable stage was integrated to account for an accurate positioning of the sample underneath the indenter.

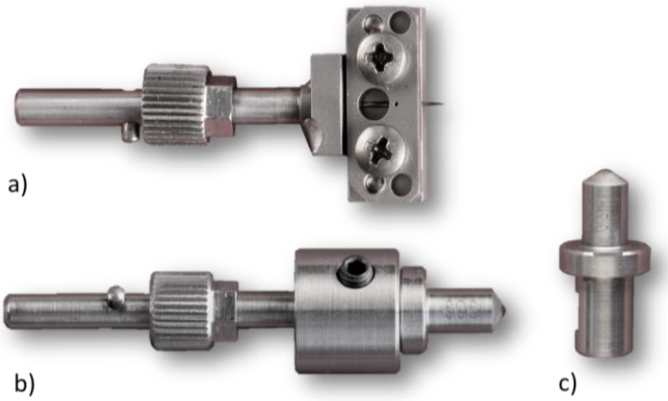

Fig. 14 Indenter holders for the DMA; a) tungsten needle indenter, b) diamond indenters with standard geometry, and c) indenter head

In the DMA indentation experiments a sinusoidal force $F(t)$ generates a periodic indentation amplitude $h(t)$ as a response signal. The measurements have shown that the indentation amplitudes of the diamond indenters looked rather sinusoidal while the needle indenter has a pronounced non-sinusoidal shape. This means that data generated by the diamond indenters can be directly introduced in [Thesis Eq. (48)] whereas the data generated by the needle indenter required more sophisticated treatment using Fourier analysis. The complex moduli determined by DMA indentation measurements show a similar change of depth-dependent properties as Vickers hardness measurements, but resolve the initial increase much better, Fig. 15.

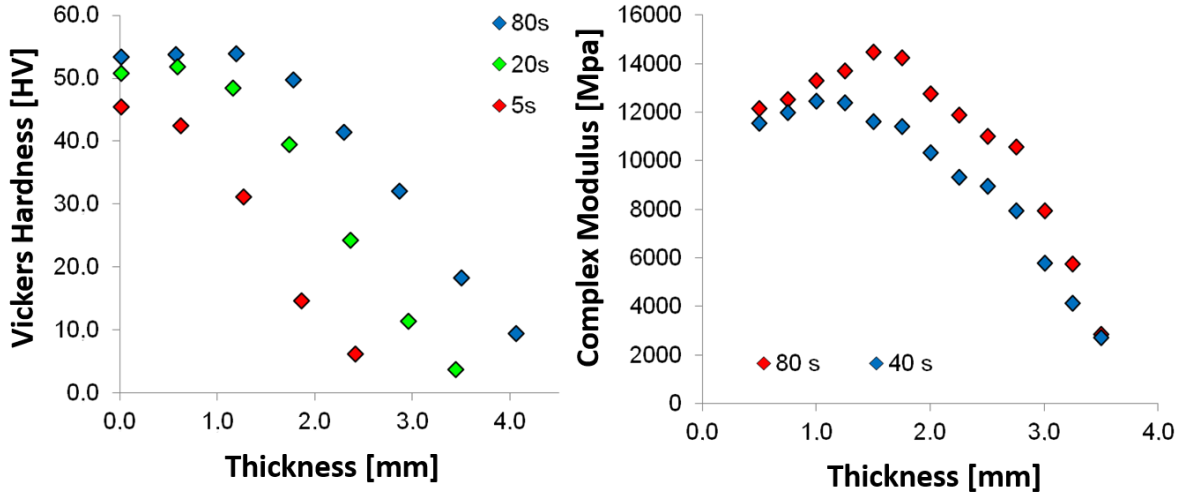

Fig. 15 hardness profile of Arabesk irradiated with Bluephase 20i Turbo (left); profile of complex modulus of Arabesk determined using DMA indentation (right)

The distribution of complex moduli is comparable to results generated by hardness mapping, Fig. 16. This verifies DMA indentation as an appropriate method to determine the local viscoelastic properties. Furthermore, as the modulus of cross-linked polymers is related to the cross-link density, it may provide the chance to determine cross-link density quantitatively.

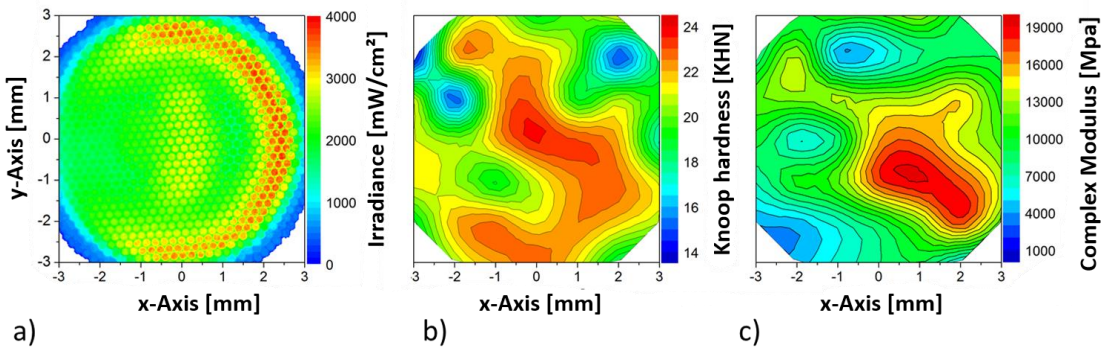

Fig. 16 Determination of the influence of the irradiance distribution a) on hardness distribution b) and distribution of complex module determined by DMA indentation c); sample: Arabesk irradiated with Bluephase 20i Turbo for 80 s

3.4 Effects of the post-curing on hardness evolution of VLC RBCs

3.4.1 Surface hardness prediction by using a master curve post-curing concept [P-VI]

During post-curing chemical and physical properties change because of a diffusion-controlled polymerization in the glassy state without any introduction of light due to trapped radicals [88]. In the reaction kinetics section, it was shown that the change from primary curing in the liquid state to post-curing in the glassy state happens after few seconds. However, as post-curing takes place over long times it can contribute remarkably to the final *DC* and further increase the mechanical properties.

During primary curing VLC RBCs are cured to a certain degree of conversion depending on the irradiance levels of LCUs and exposure times. Therefore, hardness of top and the bottom surfaces of the samples were measured for times of 10 minutes to one week after irradiation, Fig. 17. The top surface produced for all irradiances higher hardness values than the bottom surface. The interpretation of this result is that the kinetics of post-curing processes is determined by the conditions under which the liquid resin was transferred to the glassy state. At the bottom surface in a depth of 1 mm the light intensity is approximately half that at the top surface. If one assumes - according to the “total energy concept” - that radical concentration is proportional to irradiance, the cured Arabesk resin has roughly the double cross-linking density at the top surface compared to the bottom surface. Both surfaces are in glassy state, however, the molecular mobility at the bottom surface is a little bit higher due to the less cross-linked network. On first sight this should lead

to a higher rate of post-curing. However, the rate of radical annihilation is also increased, especially if further irradiation generates new radicals via initiation reactions. The decrease of radical concentration subsequently decreases the rate of post-curing. Thus, high rates of post-curing can be expected only if the cured resin consists of a highly cross-linked network, in which the radicals are bound to immobile chain ends, and hardly subjected to termination reactions.

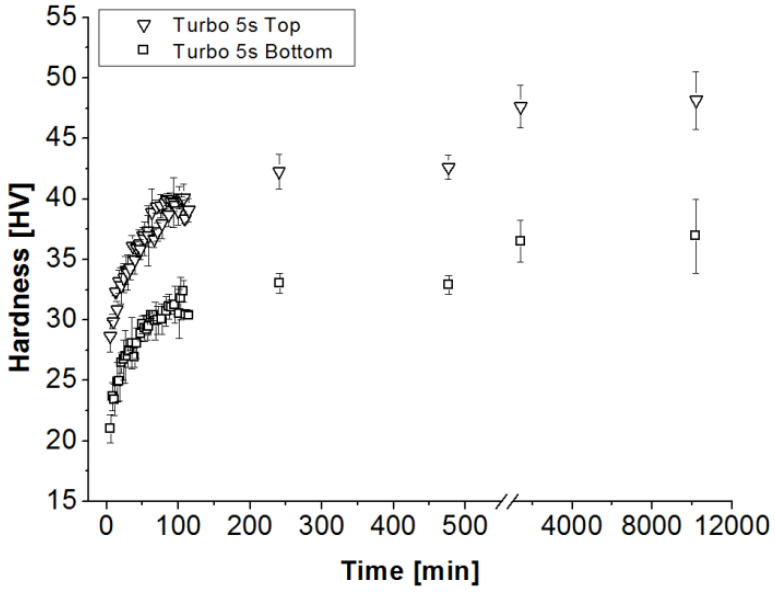

Fig. 17 Evolution of hardness for one week; Arabesk irradiated with Bluephase 20i Turbo for 5 s

Longer exposure times shift the hardness curves to higher values. The increasing hardness values seem to have a logarithmic time-dependency, and the hardness values lay on straight lines, which clearly distinguish between the top and the bottom surfaces, [P-VI Fig. 4]. On first sight, the slopes of the hardness increase on the logarithmic time scale seem to be similar for the different irradiation times. This suggests the presence of a superposition principle for the post-curing process – short term hardness values of long irradiation times correspond to long term hardness values of short irradiation times – allowing construction of a master curve using the function, Eq. (19):

$$HV\left(\lg(a_{t_{irrad}} * t)\right) = a * \lg(a_{t_{irrad}} * t) + b = a * \left(\lg t + \lg a_{t_{irrad}}\right) + b \qquad (19)$$

with Vickers hardness *HV*, shift factor $a_{t_{irrad}}$, slope *a* and intercept *b*.

Fig. 18 shows that the hardness values of different irradiation times can be shifted well to master curves, if shifted with the shift factors given in [Table 3 P-VI]. The self-similarity implies that the kinetics of post-curing is determined by a single variable of the type f(I_{LCU}, t_{irrad}).

If the master curves are fitted linearly, it is found that the slopes of the hardness of the top surface are slightly larger than those of the bottom surface, Fig. 18. The construction of master curves requires the definition of the reference measurements,

which are given by hardness curves irradiated for 20 s (Polofil Lux and Celalux) and 10 s (Bluephase 20i Turbo) as these irradiation conditions correspond to radiant exposures of approximately 20 J/cm².

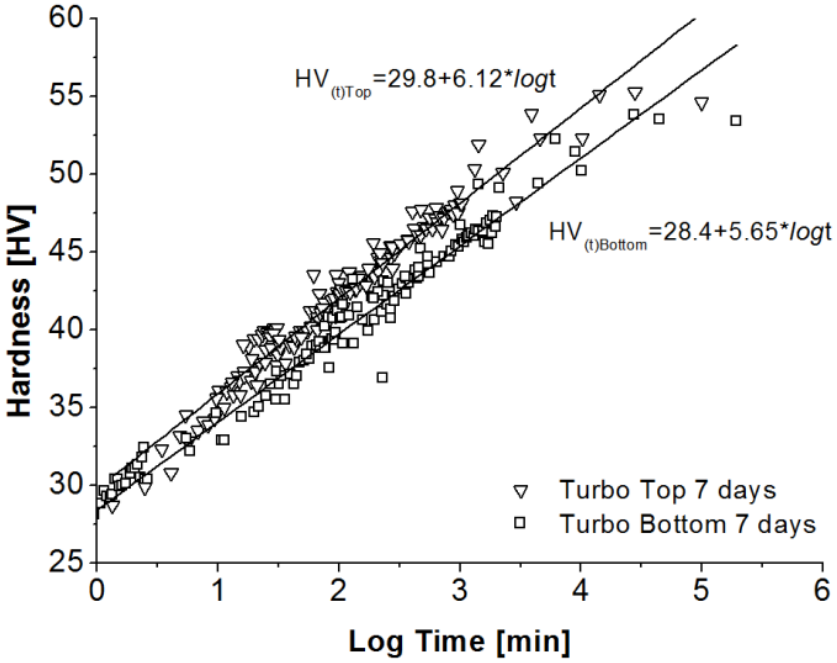

Fig. 18 Master curves of top and bottom surface hardness values with fit curves

Thus, the master curve construction is the base for predicting the post-curing state in terms of hardness, and indirectly the state of cross-linking. For Arabesk the hardness increase is predicted to be around 6 HV per decade of time. This means that the hardness would increase from 55 to 73 HV in 20 years.

4 CONCLUSIONS

In this PhD thesis the effect of the curing conditions - irradiance, exposure time and irradiance distribution of light curing units (LCUs) - on reaction kinetics as well as mechanical properties were investigated.

LCUs differ with respect to irradiance, spectrum and irradiance distribution. As this fact is not known to most dentists, their handling of LCU for curing purposes is rather arbitrary with the consequence of insufficiently cured restorations. Therefore, a simple, user-friendly method using iPad or SLR cameras was developed allowing for determining intensity distributions of LCUs.

The effects of irradiance and exposure time on reaction kinetics were investigated by FTIR-ATR to get real time degree of conversion (*DC*) data. In order to evaluate these *DC* data a novel *DC*-function was developed by the introduction of a time dependent reaction constant taking into account the slow-down of curing reactions due to the increase of both resin viscosity and its glass transition temperature. The novel *DC*-function produces intrinsically final *DC*-values less than 100 % and it shows that the curing kinetics is determined mainly by one quantity – the reaction time constant τ_{reac}^{0} – which is a function of irradiance. Furthermore, it was shown that the reaction rates – for which the reaction time constant τ_{reac}^{0} is a measure – change with the square root of the irradiance. This clearly means that the "total energy concept" fails for the considered range of irradiance. To which extent the other parameters of the novel *DC*-function – growing time constant and strength - depend on τ_{reac}^{0} has to be investigated in a future. As the *DC* is around 45 % after a time corresponding to the reaction time constant τ_{reac}^{0} , it might be considered as the time, in which the resin is transferred to the glassy state and post-curing starts.

As one focus of this PhD-thesis laid on the kinetics of post-curing both *DC* data over 160 s corresponding to 15 to 30 times τ_{reac}^{0} and hardness increase over 7 days was measured. The *DC* data showed that the "total energy concept" also failed here in the high irradiance range. The evaluation of both data sets revealed that the kinetics of post-curing can be well described by a logarithmic time dependency. Surprisingly samples cured with different irradiation times produced hardness curves during post-curing allowing for constructing master curves. It was clearly shown for the investigated composites that the post-curing kinetics differs with depth. Furthermore, the master curves can be used to predict the hardness change for really long times.

With increasing irradiances and exposure times more VLC RBC is cured. The thickness of the cured layer is measured by a quantity called depth of cure (*DoC*). Although its meaning is intuitively clear, its determination is heuristic. Therefore, a new method to determine *DoC* was proposed by measuring depth dependent changes of properties (e.g. hardness, mass loss in solvent or post-reaction enthalpy) and fitting the data with a hyperbola tangent. It turned out that the *DoC* can be

simply determined as the intercept of the plateau value close to the surface with the slope of the tangent at the inflection point. The evaluation procedure also showed that the considered property has decreased to 88 % of its initial value.

Hardness mapping of sample surfaces showed that patterns of the irradiance distribution of the LCU are reflected in the hardness distribution of the surfaces. Longer irradiation times increased the hardness values in the surface but did not surprisingly level out the patterns. This means that the pattern of hardness (and corresponding *DC*) frozen in the moment the resin transfers to the glassy state will be maintained irrespective of further irradiation.

A new indentation method based on a commercial Dynamic Mechanical Analyser (DMA) was developed to determine local viscoelastic properties of the VLC RBC. First results showed that the measured stiffness maps correspond qualitatively to their hardness maps.

5 CONTRIBUTION TO SCIENCE AND PRACTICE

Final properties such as hardness, modulus or chemical resistance of visible light curing resin based composites depend on the curing conditions. The resulting properties are important due to their influence on the resistance of dental restorations over the lifetime. Therefore, the understanding of the influences on the curing process during irradiation as well as post-curing is important to identify the right curing strategy.

In this PhD-thesis curing behavior is connected to the resulting composites properties by reaction kinetics, degree of conversion (*DC*) measurements, investigations of depth depending properties and post-curing behavior. Thus, the following points are considered as relevant contributions to science and practice:

1) The investigation of reaction kinetics of commercial dental composites showed for the first time that the curing rate depends on the square root of light curing unit (LCU) irradiance and that the “total energy concept” fails for such high irradiances. The reaction kinetics is mainly governed by the reaction time constant .
2) A novel *DC*-function was developed which intrinsically produces final *DC*-values less than 100 % and better coincidence with measured data. It also indicates that separation of primary curing and post-curing should be possible.
3) Samples irradiated with different exposure times produced hardness curves during post-curing; their master curves can be constructed allowing for long term predictions of hardness evolution.
4) For high irradiances with short curing times the “total energy concept” also fails, showing that it can only be used for LCU operated with low irradiances. Thus, if dentists use high irradiance LCUs the rule “double irradiance - halve exposure time” does not apply any longer.
5) A new method to determine the depth of cure (*DoC*) is suggested.

A dynamic mechanical indentation technique was implemented on a commercial DMA machine allowing for determining viscoelastic properties locally. Furthermore, deeper insight becomes possible as these properties can be determined as a function of temperature and frequency.

REFERENCES

[1] Ferracane JL. Resin composite--state of the art. Dent Mater, 2011; 27:29–38.
[2] Bayne SC. Beginnings of the dental composite revolution. J Am Dent Assoc, 2013; 144:880–884.
[3] Stansbury JW. Curing Dental Resins and Composites by Photopolymerization. J Esthet Restor Dent, 2000; 12:300–308.
[4] Rueggeberg FA. State-of-the-art: dental photocuring--a review. Dent Mater, 2011; 27:39–52.
[5] Peutzfeldt A. Resin composites in dentistry: the monomer systems. Eur J Oral Sci, 1997; 105:97–116.
[6] Stansbury JW. Dimethacrylate network formation and polymer property evolution as determined by the selection of monomers and curing conditions. Dent Mater, 2012; 28:13–22.
[7] Steinhaus J. Real-time Investigation of Curing Mechanisms of Thermoset Resins for Medical and Technical Applications. Dissertation. Dissertation. Zlin, 2015.
[8] Neumann MG, Miranda WG, Schmitt CC, et al. Molar extinction coefficients and the photon absorption efficiency of dental photoinitiators and light curing units. J Dent, 2005; 33:525–532.
[9] Anusavice KJ, Shen C, Rawls HR. Phillips' Science of dental materials. Saunders. Philadelphia, 2012. 9781437724189.
[10] Klapdohr S, Moszner N. New Inorganic Components for Dental Filling Composites. Monatsh Chem, 2005; 136:21–45.
[11] van Noort R. Introduction to dental materials. Mosby. Edinburgh, 2009. 0723434042.
[12] Ferracane JL. Current Trends in Dental Composites. Crit Rev Oral Biol Med, 1995; 6:302–318.
[13] Lambrechts P, Vanherle G. Structural evidences of the microfilled composites. J Biomed Mater Res, 1983; 17:249–260.
[14] Watts DC. Reaction kinetics and mechanics in photo-polymerised networks. Dent Mater, 2005; 21:27–35.
[15] Green GE, Stark BP, Zahir SA. Photocross-Linkable Resin Systems. J Macromol Sci Polym Rev, 1981; 21:187–273.
[16] Odian G. Principles of Polymerization (Fourth Edition). Wiley-Interscience. Hoboken, 2004. 0471274003.
[17] Netto AM, Steinhaus J, Hausnerova B, et al. Time-Resolved Study of the Photo-Curing Process of Dental Resins with the NMR-MOUSE. Appl Magn Reson, 2013; 44:1027–1039.
[18] Andrzejewska E. Photopolymerization kinetics of multifunctional monomers. Prog Polym Sci, 2001; 26:605–665.
[19] Beun S, Glorieux T, Devaux J, et al. Characterization of nanofilled compared to universal and microfilled composites. Dent Mater, 2007; 23:51–59.

[20] Stansbury JW, Dickens S. Determination of double bond conversion in dental resins by near infrared spectroscopy. Dent Mater, 2001; 17:71–79.
[21] Trujillo M, Newman SM, Stansbury JW. Use of near-IR to monitor the influence of external heating on dental composite photopolymerization. Dent Mater, 2004; 20:766–777.
[22] Calheiros FC, Daronch M, Rueggeberg FA, et al. Influence of irradiant energy on degree of conversion, polymerization rate and shrinkage stress in an experimental resin composite system. Dent Mater, 2008; 24:1164–1168.
[23] Moore BK, Platt JA, Borges G, et al. Depth of cure of dental resin composites: ISO 4049 depth and microhardness of types of materials and shades. Oper Dent, 2008; 33:408–412.
[24] Flury S, Hayoz S, Peutzfeldt A, et al. Depth of cure of resin composites: Is the ISO 4049 method suitable for bulk fill materials? Dent Mater, 2012; 28:521–528.
[25] Alrahlah A, Silikas N, Watts DC. Post-cure depth of cure of bulk fill dental resin-composites. Dent Mater, 2014; 30:149–154.
[26] Santos GB, Medeiros IS, Fellows CE, et al. Composite depth of cure obtained with QTH and LED units assessed by microhardness and micro-Raman spectroscopy. Oper Dent, 2007; 32:79–83.
[27] Cammann, K (Ed.). Instrumentelle analytische Chemie. Verfahren, Anwendungen und Qualitätssicherung. Spektrum Akad. Verl. Heidelberg, 2001. 3-8274-0057-0.
[28] Oréfice R, Discacciati J, Neves A, et al. In situ evaluation of the polymerization kinetics and corresponding evolution of the mechanical properties of dental composites. Polym Test, 2003; 22:77–81.
[29] Wendl B, Droschl H, Kern W. A comparative study of polymerization lamps to determine the degree of cure of composites using infrared spectroscopy. Eur J Orthod, 2004; 26:545–551.
[30] PerkinElmer. FTIR Spectroscopy: Attenuated Total Reflectance (ATR). Shelton.
[31] Larkin P. Infrared and Raman spectroscopy: Principles and spectral interpretation. Elsevier. Amsterdam, 2011. 1283114046.
[32] Bumbrah GS, Sharma RM. Raman spectroscopy – Basic principle, instrumentation and selected applications for the characterization of drugs of abuse. Egyptian J For Sci, 2015.
[33] Pianelli C, Devaux J, Bebelman S, et al. The micro-Raman spectroscopy, a useful tool to determine the degree of conversion of light-activated composite resins. J Biomed Mater Res, 1999; 48:675–681.
[34] Shin W, LI X, Schwartz B, et al. Determination of the degree of cure of dental resins using Raman and FT-Raman spectroscopy. Dent Mater, 1993; 9:317–324.
[35] Xu J, Butler IS, Gibson D, et al. High-pressure infrared and FT-Raman investigation of a dental composite. Biomaterials, 1997; 18:1653–1657.
[36] Chase DB. Fourier transform Raman spectroscopy. J Am Chem Soc, 1986; 108:7485–7488.

[37] Breschi L, Cadenaro M, Antoniolli F, et al. Polymerization kinetics of dental adhesives cured with LED: correlation between extent of conversion and permeability. Dent Mater, 2007; 23:1066–1072.
[38] Maffezzoli A, Pietra A, Rengo S, et al. Photopolymerization of dental composite matrices. Biomaterials, 1994; 15:1221–1228.
[39] Ehrenstein GW, Riedel G, Trawiel P. Thermal analysis of plastics. Theory and practice. Hanser. Munich, 2004. 9783446226739.
[40] Steinhaus J, Hausnerova B, Moeginger B, et al. Characterization of the auto-curing behavior of rapid prototyping materials for three-dimensional printing using dielectric analysis. Polym Eng Sci, 2015; 55:1485–1493.
[41] Leprince JG, Leveque P, Nysten B, et al. New insight into the "depth of cure" of dimethacrylate-based dental composites. Dent Mater, 2012; 28:512–520.
[42] Wu W, Fanconi BM. Post-curing of dental restorative resin. Polym Eng Sci, 1983; 23:704–707.
[43] Steinhaus J, Moeginger B, Grossgarten M, et al. Dielectric analysis of depth dependent curing behavior of dental resin composites. Dent Mater, 2014; 30:679–687.
[44] Rosentritt M, Shortall AC, Palin WM. Dynamic monitoring of curing photoactive resins: a methods comparison. Dent Mater, 2010; 26:565–570.
[45] Steinhaus J, Hausnerova B, Haenel T, et al. Curing kinetics of visible light curing dental resin composites investigated by dielectric analysis (DEA). Dent Mater, 2014; 30:372–380.
[46] Dielectric Cure Monitoring. Method, Technique, applications. Selb.
[47] Arikawa H, Kanie T, Fujii K, et al. Effect of inhomogeneity of light from light curing units on the surface hardness of composite resin. Dent Mater J, 2008; 27:21–28.
[48] Ferracane JL. Correlation between hardness and degree of conversion during the setting reaction of unfilled dental restorative resins. Dent Mater, 1985; 1:11–14.
[49] Price RBT, Labrie D, Rueggeberg FA, et al. Correlation between the beam profile from a curing light and the microhardness of four resins. Dent Mater, 2014; 30:1345–1357.
[50] Fischer-Cripps AC. Nanoindentation. Springer. New York, NY, 2002. 0387953949.
[51] Oliver WC, Pharr GM. An improved technique for determining hardness and elastic modulus using load and displacement sensing indentation experiments. J Mater Res, 1992; 7:1564–1583.
[52] Binnig G, Quate, Gerber. Atomic force microscope. Phys Rev Lett, 1986; 56:930–933.
[53] Salerno M, Patra N, Diaspro A. Atomic force microscopy nanoindentation of a dental restorative midifill composite. Dent Mater, 2012; 28:197–203.
[54] Jandt KD. Atomic force microscopy of biomaterials surfaces and interfaces. Surf Sci, 2001; 491:303–332.
[55] Bhushan B, Koinkar VN. Nanoindentation hardness measurements using atomic force microscopy. Appl. Phys. Lett., 1994; 64:1653.

[56] Marshall GW, Marshall SJ, Kinney JH, et al. The dentin substrate Structure and properties related to bonding. J Dent, 1997; 25:441–458.
[57] Nanovea. Mechanical Tester.
[58] Keysight Nano Indenter G200. USA.
[59] Bruker Corporation. NanoForce Nanomechanical Testing System. Enabling Nwe Discoveroes in Nanomechanics.
[60] Willems G, Celis JP, Lambrechts P, et al. Hardness and Young's modulus determined by nanoindentation technique of filler particles of dental restorative materials compared with human enamel. J Biomed Mater Res, 1993; 27:747–755.
[61] Drummond JL. Nanoindentation of Dental Composites. J Biomed Mater Res Part B Appl Biomater, 2006; 78:27–34.
[62] Willems G, Lambrechts P, Braem M, et al. A classification of dental composites according to their morphological and mechanical characteristics. Dent Mater, 1992; 8:310–319.
[63] Lin-Gibson S, Sung L, Forster AM, et al. Effects of filler type and content on mechanical properties of photopolymerizable composites measured across two-dimensional combinatorial arrays. Acta Biomater, 2009; 5:2084–2094.
[64] Mohamad D, Young RJ, Mann AB, et al. Post-polymerization of dental resin composite evaluated with nanoindentation and micro- Raman spectroscopy. Arch Orofac Sci, 2007; 2:26–31.
[65] Ho E, Marcolongo M. Effect of coupling agents on the local mechanical properties of bioactive dental composites by the nano-indentation technique. Dent Mater, 2005; 21:656–664.
[66] Naderi M, Saeed-Akbari A, Bleck W. Quantitative and qualitative investigation of the heterogeneous microstructures using surface hardness mapping and dilatation data. Mater Lett, 2008; 62:1132–1135.
[67] Grellmann W, Seidler S. Polymer Testing. Carl Hanser Fachbuchverlag. s.l., 2012. 9781569905487.
[68] Ferry JD. Viscoelastic properties of polymers. Wiley. New York, 1980. 0471048941.
[69] Ramorino G, Vetturi D, Cambiaghi D, et al. Developments in dynamic testing of rubber compounds. Polym Test, 2003; 22:681–687.
[70] Frank A, Pinter G, Lang RW. Prediction of the remaining lifetime of polyethylene pipes after up to 30 years in use. Polym Test, 2009; 28:737–745.
[71] www.open.edu/openlearn/science-maths-technology/science/chemistry/introduction-polymers/content-section-5.3.1.
[72] Emami N, Söderholm KM. Dynamic mechanical thermal analysis of two light-cured dental composites. Dent Mater, 2005; 21:977–983.
[73] Vidal Mesquita R. Dynamic mechanical analysis of dental composite resins. Dissertation. Dissertation. Tübingen.
[74] Ferracane JL, Greener EH. The effect of resin formulation on the degree of conversion and mechanical properties of dental restorative resins. J Biomed Mater Res, 1986; 20:121–131.

[75] Lovell LG, Lu H, Elliott JE, et al. The effect of cure rate on the mechanical properties of dental resins. Dent Mater, 2001; 17:504–511.
[76] Herrmann V. Charakterisierung von Elastomeren mittels dynamischer Indentation und vergleichender Methoden. Dissertation. Dissertation. Aachen, 2002.
[77] Bennett AW, Watts DC. Performance of two blue light-emitting-diode dental light curing units with distance and irradiation-time. Dent Mater, 2004; 20:72–79.
[78] D'Alpino PHP, Svizero NR, Pereira JC, et al. Influence of light-curing sources on polymerization reaction kinetics of a restorative system. Am J Dent, 2007; 20:46–52.
[79] Jandt KD, Mills RW. A brief history of LED photopolymerization. Dent Mater, 2013; 29:605–617.
[80] Aravamudhan K, Rakowski D, Fan P. Variation of depth of cure and intensity with distance using LED curing lights. Dent Mater, 2006; 22:988–994.
[81] Price RBT, Labrie D, Rueggeberg FA, et al. Irradiance differences in the violet (405 nm) and blue (460 nm) spectral ranges among dental light-curing units. J Esthet Restor Dent, 2010; 22:363–377.
[82] Nomoto R. Effect of light wavelength on polymerization of light-cured resins. Dent Mater J, 1997; 16:60–73.
[83] Price RBT, Rueggeberg FA, Labrie D, et al. Irradiance uniformity and distribution from dental light curing units. J Esthet Restor Dent, 2010; 22:86–101.
[84] Selig D, Haenel T, Hausnerová B, et al. Examining exposure reciprocity in a resin based composite using high irradiance levels and real-time degree of conversion values. Dental materials : official publication of the Academy of Dental Materials, 2015; 31:583–593.
[85] Gonçalves F, Kawano Y, Pfeifer C, et al. Influence of BisGMA, TEGDMA, and BisEMA contents on viscosity, conversion, and flexural strength of experimental resins and composites. Eur J Oral Sci, 2009; 117:442–446.
[86] Ferracane JL, Greener EH. Fourier transform infrared analysis of degree of polymerization in unfilled resins--methods comparison. J Dent Res, 1984; 63:1093–1095.
[87] Emami N, Soderholm KM. How light irradiance and curing time affect monomer conversion in light-cured resin composites. Eur J Oral Sci, 2003; 111:536–542.
[88] Peutzfeldt A, Asmussen E. Resin composite properties and energy density of light cure. Journal of dental research, 2005; 84:659–662.
[89] Leprince J, Lamblin G, Truffier-Boutry D, et al. Kinetic study of free radicals trapped in dental resins stored in different environments. Acta Biomaterialia, 2009; 5:2518–2524.

LIST OF FIGURES

LIST OF TABLES

ABBREVIATIONS

AFM	Atomic force microscopy
ATR	Attenuated total reflection
BisEMA	Ethoxylated bisphenol-A dimethacrylate
BisGMA	Bisphenol A glycidyl methacrylate
CQ	Camphorquinone
DABE	Ethyl 4-aminobenzoate
DC	Degree of conversion
DEA	Dielectric analysis
DMA	Dynamic mechanical analysis
DoC	Depth of cure
DSC	Differential scanning calorimetry
Eq.	Equation
FTIR	Fourier transformation infrared spectroscopy
HK	Knoop hardness
HM	Martens hardness
HV	Vickers harndess
LCU	Light Curing Unit
LED	Light emitted diode
MMA	Methyl methacrylate
PAC	Plasma arc
PMMA	Polymethylmethacrylate
PPD	1-Phenyl-1,2-propandedione
PPF	Pre-polmerized fillers
PS	Polystyrene
QTH	Quartz-tungsten halogen
RBC	Resin based composite
RBC	Resin based composite
SEM	Scanning electron microscope
TEGDMA	Triethylene glycol dimethacrylate
TPO	Monoacylphosphine oxid
UDMA	Urethane dimethacrylate
UV	Ultra violet
VLC	Visible light curing
VLC RBC	Visible light curing resin based composites

SYMBOLS

A	Imprint area (indentation)
$Abs_{aliphatic}$	Absorbance of aliphatic C=C-bonds
$Abs_{aromatic}$	Absorbance of aromatic C=C-bonds
c	Concentration
c_p	Heat capacity
d	Diagonal
DC	Degree of conversion
$DC(t,x)$	Time and depth dependent DC
$DC_{DEA}(t)$	Time dependent DC determined by Dielectric analysis
$DC_{DSC}(t)$	Time dependent DC determined by Differential scanning calorimetry
$DC_{IR}(t)$	Time dependent DC determined by infrared spectroscopy
E	Elastic modulus
E_t	Elastic modulus of indenter
E_s	Elastic modulus of sample
$E^*(\omega, T)$	Frequency and temperature dependent complex modulus
E'	Storage modulus
E''	Loss modulus
F	Force
ΔH	Reaction enthalpy
ΔH_{calc}	Calculated reaction enthalpy
ΔH_{obs}	Observed reaction enthalpy
HK	Knoop hardness
HM	Martens hardness
HV	Vickers hardness
h_{max}	Maximal indentation displacement
I_a	Absorbed light intensity
$I(x)$	Transmitted light at a certain thickness
I_0	Incident light intensity
k_i	Initial rate constant
k_P	Propagation rate constant
k_t	Termination rate constant
P	Load (indentation)
$\dot{Q}(t)$	Heat flow

ΔQ_{curing}	Curing heat
R_p	Rate of propagation
R_{tc}	Rate of combination
R_{td}	Rate of disproportionation
R_{pol}	Rate of polymerization (rate of reaction)
R_i	Rate of initiation
S_0	Ground state
S_n	Exited state
t	Time
t_{irr}	Irradiation time (VLC RBC kinetics)
T_g	Glass transition temperature
Tm	Melting temperature
ΔV_P	Volume contraction
x	Thickness/depth

GREEK SYMBOLS

α	Tip angle of indenter
δ	Phase angle
$tan\ \delta$	Loss factor
ε_0	Strain amplitude
ε_λ	Wavelength dependent extinction coefficient
$\varepsilon_{(\omega,t)}$	Time and frequency dependent strain (dynamic mechanical analysis)
η_0^{ion}	Initial ion viscosity
η_{min}^{ion}	Minimum ion viscosity
η_∞^{ion}	Final ion viscosity
$\eta^{ion}(t)$	Time dependent ion viscosity
λ	Wavelength
ν_s	Poisson's ratio of sample
ν_t	Poisson's ratio of indenter
σ_0	Stress amplitude
$\sigma_{(t,\omega)}$	Time and frequency dependent stress
ϕ	Quantum yield
ω	Angular frequency
ν_t	Poisson's ratio of indenter
σ_0	Stress amplitude
$\sigma_{(t,\omega)}$	Time and frequency dependent stress
ϕ	Quantum yield
ω	Angular frequency

CHEMICAL SYMBOLS

C=C	Carbon-carbon double bonds
I	Initiator molecules
[I]	Concentration of initiator
M	Monomer
Mn•	Monomer radical
[M]	Concentration of monomers
M_0	Initial Monomer concentration
R•	Radical
[R•]	Concentration of radicals
R1, R2…	Organic groups

PUBLICATIONS, POSTERS AND PRESENTATIONS

Publications in the context of this doctoral work:

- Qualitative beam profiling of light-curing units for resin based composites. T. Haenel, B. Hausnerová, J. Steinhaus, B. Moeginger. Eur J Prosthodont Rest Dent, 2016, accepted.
- Initial Reaction Kinetics of two Resin Based Dental Composites. T. Haenel, B. Hausnerová, J. Steinhaus, R. Price, B. Moeginger. Submitted to Dent Mater, July 2016.
- Examining exposure reciprocity in a resin based composite using high irradiance levels and real-time degree of conversion values. D. Selig, T. Haenel, B. Hausnerová, B. Moeginger, D. Labrie, B. Sullivan, R. Price. Dent Mater, 2015, vol. 31, 583-593.
- Determining depth of cure (*DoC*) of VLC RBC intrinsically using a new evaluation procedure to profiles of depth dependent hardness, mass loss after solvent extraction and post-reaction enthalpy. T. Haenel, B. Hausnerová, M. Dopadlo, J. Steinhaus, B. Moeginger. Submitted to Dent Mater, July 2016.
- Effect of the irradiance distribution from light curing units on the local micro-hardness of the surface of dental resins. T. Haenel, B. Hausnerová, J. Steinhaus, R.B.T. Price, B. Sullivan, B. Moeginger. Dent Mater 2015, vol. 31, 93-104.
- Post-curing induced Hardness Increase of a Light Curing Dental Composites and its modeling. T. Haenel, B. Hausnerová, L. Kehret, J. Steinhaus, B. Moeginger. Submitted to Dent Mater, August 2016.

Other Publications in English language:

- Correlation of shear and dielectric ion viscosity of dental resins – Influence of composition, temperature and filler content. J. Steinhaus, B. Hausnerová, T. Haenel, D. Selig, F. Duvenbeck, B. Moeginger. Dent Mater, 2016; 32(7): 899-907.
- Effect of a Broad-Spectrum LED Curing Light on the Knoop Microhardness of Four Posterior Resin Based Composites at 2, 4 and 6-mm Depths. M. Alshaafi, T. Haenel, B. Sullivan, D. Labrie, M. Alqahtani, R.B.T. Price. J Dent, 2016; 45:14-18.
- Curing Kinetics of Visible Light Curing Dental Resin Composites Investigated by Dielectric Analysis (DEA). J. Steinhaus, B. Hausnerová, T. Haenel, M. Großgarten, B. Moeginger. Dent Mater. 2014; 30(3): 837-380.

Conference Presentations:

- A New Evaluation Method to Determine Depth Depending Properties of Visible Light Curing Resin Based Composites. T. Haenel, M. Dopadlo, R.B.T. Price, B. Hausnerová, J. Steinhaus, Esther van Dorp, B. Moeginger. 2015, IADR (International Association for Dental Research), Antalya, Turkey, oral poster presentation
- A New Approach to Model Thermal Expansion of Semi Crystalline Polymers. E. van Dorp, T. Haenel, J. Steinhaus, D. Reith, O. Bruch, B. Hausnerová, B. Moeginger. 2015. PPS 2015
- Modeling curing kinetics and degree of conversion of visible light curing resin based composites (VLC RBC) using a time dependent reaction constant. B. Moeginger, T. Haenel, J. Steinhaus, B. Hausnerová, R.B.T. Price. 2015; European Dental Materials, Nürnberg, Germany, oral poster presentation.
- Effect of composition on the curing behaviour of visible light-curing resins measured with dielectric analysis. J. Steinhaus, D- Selig, T. Haenel, B. Moeginger, B. Hausnerová. 2015. European Dental Materials, Nürnberg, Germany, oral poster presentation.
- Effect of Thickness on the Properties of Bulk Cured Resins. M. Alshaafi, M.Q. Alqahtani, T. Haenel, R.B.T. Price, J. Fahey. 2013; IADR Seattle, poster presentation.
- Real-time observation of the degree of conversion of dental resins having a wide range of CQ-concentrations using ATR-FTIR. T. Haenel, R.B.T. Price, D. Labrie, B. Moeginger, J. Steinhaus, B. Hausnerová. 2012. AODES (Academy of Operative Dentistry), Leuven, Belgium. poster presentation.
- Hardness Mapping of Light-Cured Composites to Identify Inhomogeneous Curing. T. Haenel, B. Hausnerová, L. Kehret, J. Steinhaus, B. Moeginger. IADR 2011, Budapest, Hungary.

CURRICULUM VITAE

Date and place of birth	February 20th, 1980 Remscheid, Germany
Permanent Adress	von-Liebig-Str. 20
	53359 Rheinbach
	Phone: (+49) 2241 865 766
	e-mail: thomas.haenel@h-brs.de

Education

since 09/2010	PhD studies at: Tomas Bata University Zlín, Faculty of Technology,
09/2007 – 02/2010	Master studies "Applied Polymer Science" at: FH Aachen, University of Sciences
09/2003 – 07/2007	Bachelor studies "Chemistry and Material Sciences" at FH Bonn-Rhein-Sieg, University of Applied Sciences
09/1996-01/2000	Vocational education Aircraft mechanics at: 15th German Army Aviator Battalion, Rheine, Germany

Work Experience

since 09/2010	Bonn-Rhein-Sieg University of Applied Sciences, Rheinbach, Germany, Dept. of Natural Sciences, Scientific Assistance research group "Polymer Materials"
02/2008-08/2009	German Aerospace Center, Cologne, Germany, Research Assistance, Institute of Material Physics in Space,
01/2001-07/2002	Express Airways, Troisdorf, Germany, Maintenance Aircraft mechanic,
03/2000-12/2000	Military Service at: 15th German Army Aviator Battalion, Rheine, Germany

References

[1] Ferracane JL. Resin composite--state of the art. Dent Mater, 2011; 27:29–38.
[2] Bayne SC. Beginnings of the dental composite revolution. J Am Dent Assoc, 2013; 144:880–884.
[3] Stansbury JW. Curing Dental Resins and Composites by Photopolymerization. J Esthet Restor Dent, 2000; 12:300–308.
[4] Rueggeberg FA. State-of-the-art: dental photocuring--a review. Dent Mater, 2011; 27:39–52.
[5] Peutzfeldt A. Resin composites in dentistry: the monomer systems. Eur J Oral Sci, 1997; 105:97–116.
[6] Stansbury JW. Dimethacrylate network formation and polymer property evolution as determined by the selection of monomers and curing conditions. Dent Mater, 2012; 28:13–22.
[7] Steinhaus J. Real-time Investigation of Curing Mechanisms of Thermoset Resins for Medical and Technical Applications. Dissertation. Dissertation. Zlin, 2015.
[8] Neumann MG, Miranda WG, Schmitt CC, Rueggeberg FA and Correa IC. Molar extinction coefficients and the photon absorption efficiency of dental photoinitiators and light curing units. J Dent, 2005; 33:525–532.
[9] Anusavice KJ, Shen C and Rawls HR. Phillips' Science of dental materials. Philadelphia, 2012.
[10] Klapdohr S and Moszner N. New Inorganic Components for Dental Filling Composites. Monatsh Chem, 2005; 136:21–45.
[11] van Noort R. Introduction to dental materials. Edinburgh, 2009.
[12] Ferracane JL. Current Trends in Dental Composites. Crit Rev Oral Biol Med, 1995; 6:302–318.
[13] Lambrechts P and Vanherle G. Structural evidences of the microfilled composites. J Biomed Mater Res, 1983; 17:249–260.
[14] Watts DC. Reaction kinetics and mechanics in photo-polymerised networks. Dent Mater, 2005; 21:27–35.
[15] Green GE, Stark BP and Zahir SA. Photocross-Linkable Resin Systems. J Macromol Sci Polym Rev, 1981; 21:187–273.
[16] Odian G. Principles of Polymerization (Fourth Edition). Hoboken, 2004.
[17] Netto AM, Steinhaus J, Hausnerova B, Moeginger B and Blümich B. Time-Resolved Study of the Photo-Curing Process of Dental Resins with the NMR-MOUSE. Appl Magn Reson, 2013; 44:1027–1039.
[18] Andrzejewska E. Photopolymerization kinetics of multifunctional monomers. Prog Polym Sci, 2001; 26:605–665.
[19] Beun S, Glorieux T, Devaux J, Vreven J and Leloup G. Characterization of nanofilled compared to universal and microfilled composites. Dent Mater, 2007; 23:51–59.
[20] Stansbury JW and Dickens S. Determination of double bond conversion in dental resins by near infrared spectroscopy. Dent Mater, 2001; 17:71–79.

[21] Trujillo M, Newman SM and Stansbury JW. Use of near-IR to monitor the influence of external heating on dental composite photopolymerization. Dent Mater, 2004; 20:766–777.
[22] Calheiros FC, Daronch M, Rueggeberg FA and Braga RR. Influence of irradiant energy on degree of conversion, polymerization rate and shrinkage stress in an experimental resin composite system. Dent Mater, 2008; 24:1164–1168.
[23] Moore BK, Platt JA, Borges G, Chu T-MG and Katsilieri I. Depth of cure of dental resin composites: ISO 4049 depth and microhardness of types of materials and shades. Oper Dent, 2008; 33:408–412.
[24] Flury S, Hayoz S, Peutzfeldt A, Hüsler J and Lussi A. Depth of cure of resin composites: Is the ISO 4049 method suitable for bulk fill materials? Dent Mater, 2012; 28:521–528.
[25] Alrahlah A, Silikas N and Watts DC. Post-cure depth of cure of bulk fill dental resin-composites. Dent Mater, 2014; 30:149–154.
[26] Santos GB, Medeiros IS, Fellows CE, Muench A and Braga RR. Composite depth of cure obtained with QTH and LED units assessed by microhardness and micro-Raman spectroscopy. Oper Dent, 2007; 32:79–83.
[27] Oréfice R, Discacciati J, Neves A, Mansur H and Jansen W. In situ evaluation of the polymerization kinetics and corresponding evolution of the mechanical properties of dental composites. Polym Test, 2003; 22:77–81.
[28] Wendl B, Droschl H and Kern W. A comparative study of polymerization lamps to determine the degree of cure of composites using infrared spectroscopy. Eur J Orthod, 2004; 26:545–551.
[29] Cammann, K (Ed.). Instrumentelle analytische Chemie. Verfahren, Anwendungen und Qualitätssicherung. Heidelberg, 2001.
[30] PerkinElmer. FTIR Spectroscopy: Attenuated Total Reflectance (ATR). Shelton.
[31] Larkin P. Infrared and Raman spectroscopy: Principles and spectral interpretation. Amsterdam, 2011.
[32] Bumbrah GS and Sharma RM. Raman spectroscopy – Basic principle, instrumentation and selected applications for the characterization of drugs of abuse. Egyptian J For Sci, 2015.
[33] Pianelli C, Devaux J, Bebelman S and Leloup G. The micro-Raman spectroscopy, a useful tool to determine the degree of conversion of light-activated composite resins. J Biomed Mater Res, 1999; 48:675–681.
[34] Shin W, LI X, Schwartz B, Wunder S and Baran G. Determination of the degree of cure of dental resins using Raman and FT-Raman spectroscopy. Dent Mater, 1993; 9:317–324.
[35] Xu J, Butler IS, Gibson D and Stangel I. High-pressure infrared and FT-Raman investigation of a dental composite. Biomaterials, 1997; 18:1653–1657.
[36] Chase DB. Fourier transform Raman spectroscopy. J Am Chem Soc, 1986; 108:7485–7488.
[37] Breschi L, Cadenaro M, Antoniolli F, Sauro S, Biasotto M, Prati C, Tay FR and Di Lenarda R. Polymerization kinetics of dental adhesives cured with LED:

correlation between extent of conversion and permeability. Dent Mater, 2007; 23:1066–1072.
[38] Maffezzoli A, Pietra A, Rengo S, Nicolais L and Valletta G. Photopolymerization of dental composite matrices. Biomaterials, 1994; 15:1221–1228.
[39] Ehrenstein GW, Riedel G and Trawiel P. Thermal analysis of plastics. Theory and practice. Munich, 2004.
[40] Steinhaus J, Hausnerova B, Moeginger B, Harrach M, Guenther D and Moegele F. Characterization of the auto-curing behavior of rapid prototyping materials for three-dimensional printing using dielectric analysis. Polym Eng Sci, 2015; 55:1485–1493.
[41] Leprince JG, Leveque P, Nysten B, Gallez B, Devaux J and Leloup G. New insight into the "depth of cure" of dimethacrylate-based dental composites. Dent Mater, 2012; 28:512–520.
[42] Wu W and Fanconi BM. Post-curing of dental restorative resin. Polym Eng Sci, 1983; 23:704–707.
[43] Dielectric Cure Monitoring. Method, Technique, applications. Selb, 2015.
[44] Steinhaus J, Moeginger B, Grossgarten M, Rosentritt M and Hausnerova B. Dielectric analysis of depth dependent curing behavior of dental resin composites. Dent Mater, 2014; 30:679–687.
[45] Rosentritt M, Shortall AC and Palin WM. Dynamic monitoring of curing photoactive resins: a methods comparison. Dent Mater, 2010; 26:565–570.
[46] Steinhaus J, Hausnerova B, Haenel T, Großgarten M and Moeginger B. Curing kinetics of visible light curing dental resin composites investigated by dielectric analysis (DEA). Dent Mater, 2014; 30:372–380.
[47] Arikawa H, Kanie T, Fujii K, Takahashi H and Ban S. Effect of inhomogeneity of light from light curing units on the surface hardness of composite resin. Dent Mater J, 2008; 27:21–28.
[48] Ferracane JL. Correlation between hardness and degree of conversion during the setting reaction of unfilled dental restorative resins. Dent Mater, 1985; 1:11–14.
[49] Price RBT, Labrie D, Rueggeberg FA, Sullivan B, Kostylev I and Fahey J. Correlation between the beam profile from a curing light and the microhardness of four resins. Dent Mater, 2014; 30:1345–1357.
[50] Oliver WC and Pharr GM. An improved technique for determining hardness and elastic modulus using load and displacement sensing indentation experiments. J Mater Res, 1992; 7:1564–1583.
[51] Binnig G, Quate and Gerber. Atomic force microscope. Phys Rev Lett, 1986; 56:930–933.
[52] Salerno M, Patra N and Diaspro A. Atomic force microscopy nanoindentation of a dental restorative midifill composite. Dent Mater, 2012; 28:197–203.
[53] Jandt KD. Atomic force microscopy of biomaterials surfaces and interfaces. Surf Sci, 2001; 491:303–332.
[54] Bhushan B and Koinkar VN. Nanoindentation hardness measurements using atomic force microscopy. Appl. Phys. Lett., 1994; 64:1653.

[55] Marshall GW, Marshall SJ, Kinney JH and Balooch M. The dentin substrate Structure and properties related to bonding. J Dent, 1997; 25:441–458.
[56] Nanovea. Mechanical Tester.
[57] Keysight Nano Indenter G200. USA, 2014.
[58] Bruker Corporation. NanoForce Nanomechanical Testing System. Enabling Nwe Discoveroes in Nanomechanics, 2015.
[59] Willems G, Celis JP, Lambrechts P, Braem M and Vanherle G. Hardness and Young's modulus determined by nanoindentation technique of filler particles of dental restorative materials compared with human enamel. J Biomed Mater Res, 1993; 27:747–755.
[60] Drummond JL. Nanoindentation of Dental Composites. J Biomed Mater Res Part B Appl Biomater, 2006; 78:27–34.
[61] Willems G, Lambrechts P, Braem M, Celis JP and Vanherle G. A classification of dental composites according to their morphological and mechanical characteristics. Dent Mater, 1992; 8:310–319.
[62] Lin-Gibson S, Sung L, Forster AM, Hu H, Cheng Y and Lin NJ. Effects of filler type and content on mechanical properties of photopolymerizable composites measured across two-dimensional combinatorial arrays. Acta Biomater, 2009; 5:2084–2094.
[63] Mohamad D, Young RJ, Mann AB and Watts DC. Post-polymerization of dental resin composite evaluated with nanoindentation and micro- Raman spectroscopy. Arch Orofac Sci, 2007; 2:26–31.
[64] Ho E and Marcolongo M. Effect of coupling agents on the local mechanical properties of bioactive dental composites by the nano-indentation technique. Dent Mater, 2005; 21:656–664.
[65] Naderi M, Saeed-Akbari A and Bleck W. Quantitative and qualitative investigation of the heterogeneous microstructures using surface hardness mapping and dilatation data. Mater Lett, 2008; 62:1132–1135.
[66] Grellmann W and Seidler S. Polymer Testing. s.l., 2012.
[67] Ferry JD. Viscoelastic properties of polymers. New York, 1980.
[68] Ramorino G, Vetturi D, Cambiaghi D, Pegoretti A and Ricco T. Developments in dynamic testing of rubber compounds. Assessment of non-linear effects. Polym Test, 2003; 22:681–687.
[69] Frank A, Pinter G and Lang RW. Prediction of the remaining lifetime of polyethylene pipes after up to 30 years in use. Polym Test, 2009; 28:737–745.
[70] Emami N and Söderholm K-JM. Dynamic mechanical thermal analysis of two light-cured dental composites. Dent Mater, 2005; 21:977–983.
[71] Vidal Mesquita R. Dynamic mechanical analysis of dental composite resins. Dissertation. Dissertation. Tübingen, 2006.
[72] Ferracane JL and Greener EH. The effect of resin formulation on the degree of conversion and mechanical properties of dental restorative resins. J Biomed Mater Res, 1986; 20:121–131.
[73] Lovell LG, Lu H, Elliott JE, Stansbury JW and Bowman CN. The effect of cure rate on the mechanical properties of dental resins. Dent Mater, 2001; 17:504–511.

[74] Herrmann V. Charakterisierung von Elastomeren mittels dynamischer Indentation und vergleichender Methoden. Dissertation. Dissertation. Aachen, 2002.
[75] OpenLearn. Introduction to polymers. www.open.edu/openlearn/science-maths-technology/science/chemistry/introduction-polymers/content-section-5.3.1, 2/13/2016.
[76] Bennett AW and Watts DC. Performance of two blue light-emitting-diode dental light curing units with distance and irradiation-time. Dent Mater, 2004; 20:72–79.
[77] D'Alpino PHP, Svizero NR, Pereira JC, Rueggeberg FA, Carvalho RM and Pashley DH. Influence of light-curing sources on polymerization reaction kinetics of a restorative system. Am J Dent, 2007; 20:46–52.
[78] Jandt KD and Mills RW. A brief history of LED photopolymerization. Dent Mater, 2013; 29:605–617.
[79] Aravamudhan K, Rakowski D and Fan P. Variation of depth of cure and intensity with distance using LED curing lights. Dent Mater, 2006; 22:988–994.
[80] Price RBT, Labrie D, Rueggeberg FA and Felix CM. Irradiance differences in the violet (405 nm) and blue (460 nm) spectral ranges among dental light-curing units. J Esthet Restor Dent, 2010; 22:363–377.
[81] Nomoto R. Effect of light wavelength on polymerization of light-cured resins. Dent Mater J, 1997; 16:60–73.
[82] Price RBT, Rueggeberg FA, Labrie D and Felix CM. Irradiance uniformity and distribution from dental light curing units. J Esthet Restor Dent, 2010; 22:86–101.
[83] Selig D, Haenel T, Hausnerová B, Moeginger B, Labrie D, Sullivan B and Price, Richard B T. Examining exposure reciprocity in a resin based composite using high irradiance levels and real-time degree of conversion values. Dental materials : official publication of the Academy of Dental Materials, 2015; 31:583–593.
[84] Gonçalves F, Kawano Y, Pfeifer C, Stansbury JW and Braga RR. Influence of BisGMA, TEGDMA, and BisEMA contents on viscosity, conversion, and flexural strength of experimental resins and composites. Eur J Oral Sci, 2009; 117:442–446.
[85] Ferracane JL and Greener EH. Fourier transform infrared analysis of degree of polymerization in unfilled resins--methods comparison. J Dent Res, 1984; 63:1093–1095.
[86] Emami N and Soderholm K-JM. How light irradiance and curing time affect monomer conversion in light-cured resin composites. Eur J Oral Sci, 2003; 111:536–542.
[87] Peutzfeldt A and Asmussen E. Resin composite properties and energy density of light cure. Journal of dental research, 2005; 84:659–662.
[88] Leprince J, Lamblin G, Truffier-Boutry D, Demoustier-Champagne S, Devaux J, Mestdagh M and Leloup G. Kinetic study of free radicals trapped in dental resins stored in different environments. Acta Biomaterialia, 2009; 5:2518–2524.

Thomas Haenel M.Sc.

Vytvrzování dentálních materiálů

Curing of Visible Light Curing Resin Based Dental Composites

Doctoral Thesis Summary

Published by: Tomas Bata University in Zlín,
nám. T. G. Masaryka 5555, 760 01 Zlín.

Number of copies: 30
Typesetting by: Thomas Haenel M.Sc.
This publication underwent no proof reading or editorial review.

Publication year: 2016

ISBN 978-80-…….